European Cells and Materials Vol.51 2025 (pages 1–30) DOI: 10.22203/eCM.v051a01 ISSN 1473-2262

Original Article

INVESTIGATION OF THE SAFETY AND THERAPEUTIC EFFICACY OF AXONAL DIEBACK COMPOUNDS IN A RAT MODEL OF DISC-ASSOCIATED LOW BACK PAIN

F. Lee[1], S.M. Caparaso[1], C.J. Cruz[2], E.C. Barnett[1], K.D. Allen[2] and R.A. Wachs[1,3,*]

[1]Department of Biological Systems Engineering, University of Nebraska-Lincoln, Lincoln, NE 68508, USA
[2]J. Crayton Pruitt Family Department of Biomedical Engineering, Biomedical Sciences Building, University of Florida, Gainesville, FL 32603, USA
[3]Arizona State University, School of Biological and Health Systems Engineering, Tempe, AZ 85287-9709, USA

Abstract

Introduction: Low back pain (LBP) is a global health issue and the primary cause of disability. The majority of LBP cases are associated with intervertebral disc degeneration and aberrant nerve growth into the discs. The correlation between presence of nerve fibers in degenerated discs and disc-associated LBP suggests that fiber removal could reverse the pain. Due to the neurodegenerative effects of pyridoxine and vincristine, we hypothesized that these compounds can be repurposed to induce local axonal dieback within the disc and alleviate pain. **Methods:** Two studies were conducted to test the safety and efficacy of these compounds. A safety study involved injecting pyridoxine and vincristine directly into rat L5–L6 lumbar discs and revealed no adverse effects on the animals' general health. Using a female rat model of disc-associated LBP, the efficacy of pyridoxine and vincristine was assessed through pain-like behavior assays. **Results:** Disc scrape injury induced disc degeneration, axial hypersensitivity, and aberrant nerve sprouting, but did not significantly impact open field test behaviors and gait. While both compounds partially alleviated axial hypersensitivity, only pyridoxine reduced nerve fiber staining in the disc. The amount of nerve fibers in the disc were correlated significantly with the degree of axial hypersensitivity. Gene expression analysis of dorsal root ganglia indicated upregulation of nociceptive ion channels and proinflammatory mediators after disc injury, and only vincristine reduced neural sensitization and inflammation. **Conclusions:** The findings suggest that pyridoxine and vincristine are safe for intradiscal use and may hold potential as treatments for disc-associated LBP, offering a promising avenue for treatment.

Keywords: Low back pain, intervertebral disc degeneration, nerve, pain, denervation, axonal dieback, dorsal root ganglia.

***Address for correspondence**: R.A. Wachs, Arizona State University, School of Biological and Health Systems Engineering, Tempe, AZ 85287-9709, USA. E-mail: rebecca.wachs@asu.edu.

Introduction

Low back pain (LBP) is a widespread condition affecting around 84 % of adults at some points in their lives [1] and is a leading cause for disability [2]. Chronic LBP, experienced by 10 to 15 % of LBP [1], severely impacts quality of life and increases risk of unemployment [3] and comorbidities like depression, anxiety, and sleep disorders [4]. Current treatments mainly rely on pain medications, but they offer short-term relief [5] and may have side effects [6]. Non-steroidal anti-inflammatory drugs (NSAIDs) have become a widely accepted class of pain medication for LBP patients due to its therapeutic ability to alleviate pain and inflammation [7]. However, prolonged use of NSAIDs could lead to complications such as gastrointestinal bleeding, stomach ulcers [8–10], kidney dysfunction [11] or heart failure [12,13]. Another class of pain medication is opioids, which are the most commonly prescribed drug among LBP patients [14]. Despite the increasing trends of opioid use, there is no evidence suggesting the long-term safety and effectiveness of opioid medications for chronic LBP [15]. Further, there is a concern for potential misuse, addiction, tolerance and death due to overdose when using opioids [16]. Fusion surgery, as a last resort, is invasive, costly, and can exacerbate adjacent level disc degeneration [17]. Due to the widespread prevalence of LBP, the substantial economic and workplace impact, and the limited success of existing treatments, there is a critical need for more effective, long-term solutions to treat LBP.

Intervertebral disc degeneration is closely associated to most LBP diagnoses [18–20]. Healthy discs are primarily aneural, but due to injury and/or aging, discs can degenerate causing breakdown of disc matrix and loss of

neuro-inhibitory proteoglycans which promote nerve fiber ingrowth [21,22]. Nerve fiber presence in degenerated discs is highly correlated to disc-associated LBP [18–20]. Immunohistochemical analysis of discs from LBP patients revealed that all the painful degenerated discs exhibited nerve ingrowth and 75 % of the disc samples had C-fiber nociceptors [23]. Stimulation of these nociceptors, or pain-sensing neurons, induces pain sensation [24–26]. Therefore, it is hypothesized that removing the aberrant nerves in degenerated discs may mitigate pain.

Axonal dieback compounds that specifically induce nerve fiber degeneration have the potential to treat pain by ablating nerve fiber endings. Capsaicin, found in chili peppers, binds to the Transient receptor potential vanilloid 1 (*TRPV1*) receptor, leading to nerve fiber degeneration of C-fibers and is associated with pain relief [27–30]. Capsaicin patches are approved by the United States Food and Drug Administration (FDA) for various painful conditions [31–33], and clinical trials show promise in using local capsaicin injections for pain associated with aberrant nerve growth such as in Morton's neuroma [34] and knee osteoarthritis [35,36]. However, the effectiveness of capsaicin treatments is short-lived, lasting only 18 weeks in a human clinical study of knee pain [35] and intense burning pain is a commonly reported adverse effect after capsaicin application [34,35]. For disc-associated LBP, methylene blue injection has been explored as a potential treatment by claiming to damage nerve fibers in the disc. Methylene blue is neurotoxic [37] and has anti-nociceptive and anti-inflammatory [38,39] properties, but the efficacy of treating disc-associated LBP is low and remains controversial due to conflicting results in clinical studies [40,41]. Further, *in vitro* studies have demonstrated that methylene blue is highly toxic to viability of primary rat nucleus pulposus (NP) [42] and annulus fibrosus (AF) cells [43]. Hence, there is still a need in the field to identify compounds that can safely and consistently induce axonal dieback without off target effects, to advance the development of treatments for disc-associated LBP.

Pyridoxine (Pyr), commonly known as vitamin B6, is used as a dietary supplement and to treat seizures [44], premenstrual syndrome [45], and peripheral neuropathy [46]. A clinical report [47] and *in vivo* studies have shown that high levels of Pyr consumption lead to sensory neuropathy and axonal degeneration, with subcutaneous Pyr injections in larger animals causing similar axon damage [48] and altered neuronal cytoskeleton in nerve fibers [49]. Research behind the mechanism of Pyr-induced axonal degeneration is still ongoing, but one potential mechanism for Pyr-induced axon degeneration is the disruption of gamma-aminobutyric acid (GABA) signaling causing excess depolarization of neurons and calcium release which can lead to axonal degeneration [50]. Vincristine (Vcr) is used as a chemotherapeutic to treat acute lymphoblastic leukemia, lymphomas, sarcomas and neuroblastomas [51]. Vcr binds to β-tubulin, disrupting microtubules and impairing axonal transport [52,53], which leads to nerve fiber degeneration and damage to Schwann cells [54–56]. This axon degeneration is mediated by sterile alpha and toll/interleukin-1 receptor motif-containing 1 (SARM1) activation and the mitogen-activated protein kinase (MAPK) pathway [57]. At high and prolonged doses, both Pyr and Vcr can lead to neurodegeneration [47–49,58] and development of numbness and tingling sensations in the extremities [47,51,59,60]. Previous work in our lab has identified Pyr and Vcr as suitable axonal dieback compounds by demonstrating robust axonal degeneration without dorsal root ganglion (DRG) cytotoxicity in an *in vitro* rat DRG explant culture platform [61]. We also determined that these compounds are cytocompatible human NP cells [61].

The objective of this work is to assess the safety and pain alleviation efficacy of intradiscal Pyr and Vcr injections in our *in vivo* model of disc-associated LBP [62], by disc denervation. Herein we conducted a safety evaluation by administering intradiscal injections of either Pyr or Vcr into healthy rat lumbar discs. Assessment of safety was based on the observation of factors such as animal weight, behaviors, and disc histology. After determining each compound's safety, the efficacy of Pyr and Vcr at alleviating axial hypersensitivity was evaluated in our established rat model of disc-associated LBP [62]. Grip strength, open field test and gait measurements were performed to determine evoked and movement-evoked pain-like behaviors, and micro-computed tomography (μCT) to assess longitudinal progression of disc degeneration. Immunohistochemical and histological analysis of the disc was employed to label nerves in the disc and study the effect on disc degeneration post-intervention. The results from this study suggest that intradiscal Pyr and Vcr injections are safe and lead to partial alleviation of axial hypersensitivity.

Methods

Animals

Sixty female Sprague Dawley rats (Envigo, Indianapolis, IN, USA) were housed with a 12-hour light/dark cycle and ad libitum access to food and water. All animals were acclimated to handling and behavior equipment for 6 weeks. All animals were weighed daily in the safety study and on a bi-weekly basis in the efficacy study to monitor the animal's general well-being. Weight loss greater than 10 % from the previous recording was flagged, veterinary consultation was conducted, and the animal's behavioral data were excluded from analysis as stated below.

Axonal Dieback Compound Preparation

Pyr and Vcr concentrations were selected based on previous work screening compounds for axonal dieback in rat DRG explants and cytotoxicity in DRGs and human NP cells [61]. Pyr above 500 μM and Vcr above 100 nM induced robust axonal dieback within 3 days *in vitro* with

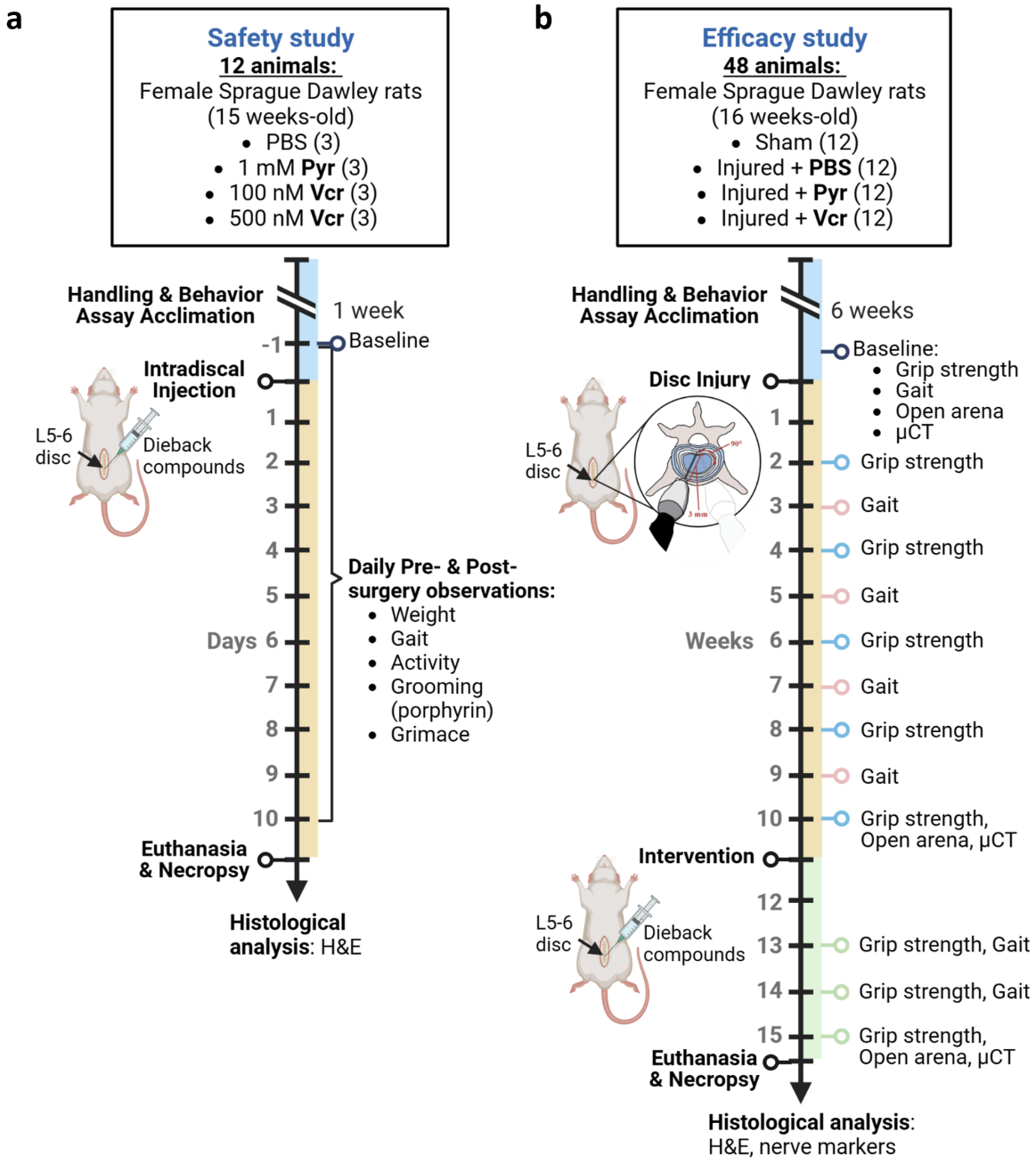

Fig. 1. Overview of studies. Animal cohort and timeline of (**a**) safety study and (**b**) efficacy study. Created with https://www.biorender.com. PBS, phosphate-buffered saline; Pyr, pyridoxine; Vcr, vincristine; H&E, hematoxylin and eosin; μCT, micro-computed tomography.

limited cytotoxicity [61]. Therefore, Pyr (1 mM) and Vcr (100 nM, 500 nM) were selected for the *in vivo* safety study. To prepare the injectable drug solutions, pyridoxine hydrochloride (Sigma Aldrich, P6280-10G) and vincristine sulfate (Sigma Aldrich, V8879-5MG) were weighed, dissolved, and diluted in 1X sterile phosphate-buffered saline (PBS) to 1.66X the desired concentration, so that the final concentration in the disc reaches 1 mM Pyr, 100 nM Vcr and 500 nM Vcr, respectively. Calculations consider the injection volume set to 2.5 μL and the approximated disc volume to be 4.15 μL as determined using μCT analysis. Solutions were prepared fresh and used on the same day.

Safety Study

Special consideration was given to develop a safe intradiscal injection procedure without leakage or extrusion of the axonal dieback compounds from the disc given the proximity of the disc to major nerve roots and the spinal

cord. Accidental injection of Vcr into the intrathecal space should be avoided as it can lead to paralysis or death [63,64]. Therefore, the safety and potential risks of intradiscal injection of axonal dieback compounds were assessed first. Twelve animals, 15-week-old female Sprague Dawley rats, were included in the safety study and randomly assigned into four groups of equal size (n = 3): 1X PBS, 1 mM Pyr, 100 nM Vcr and 500 nM Vcr (Fig. 1**a**). The animals in each group of the safety study were triple housed in the same cage.

Surgical Procedure and Intradiscal Axonal Dieback Compound Injection

On the day of surgery, rats were anesthetized with 2–3 % isoflurane in oxygen and administered subcutaneously with Buprenorphine SR (0.75 mg/kg) once for post-operative (op) pain. Dissection and visualization of the disc was performed as previously detailed [62]. Briefly, the iliac crest was used as a landmark to identify the level of the L5–L6 disc. The abdominal skin was shaved and cleaned with betadine and iodine solution. A midline incision was made along the ventral surface of the abdomen perpendicular to the level of the iliac crest, using a scalpel. The incision was continued through the skin, subcutaneous tissue, and fascia, with care taken to avoid any major blood vessels to expose the abdominal cavity and retroperitoneum. The L5–L6 disc was visualized and injected with 2.5 μL of either PBS or axonal dieback compounds (1 mM Pyr, 100 nM Vcr, 500 nM Vcr) using a 33 G needle (Air-Tite, Virginia Beach, VA, USA, TSK3313) with depth set to 2.5 mm and GasTight 1700 microsyringe (Hamilton, Reno, NV, USA, 80001) for 55 to 60 seconds (0.04–0.05 μL/second) to minimize damage, leakage, and pressurization of the disc. To ensure that the solution was fully expelled, the microsyringe remained within the disc for an extra 30 seconds before being slowly withdrawn. A dot of VetBond Tissue Adhesive (3M, St. Paul, MN, USA, sc-361931) was applied on the disc at the injection site after retracting the needle to prevent extravasation. A continuous subcuticular suture closure pattern was employed to close the abdominal wall and skin incision. Animals were monitored for 1 hour post-operatively.

General Health and Pain Assessments

To monitor the effect of axonal dieback compound injections on the rat's general health and pain in the safety study, the animals' activity and wound healing were monitored every 12 hours post-op for 3 days and observational behavioral patterns such as activity levels, gait, grimace, puffing, porphyrin staining and pain-like features (back arching, writhing, and twitching) were assessed daily for 10 days after surgery (Fig. 1**a**). During behavior assessment, the animals from each group were removed from their cage and placed on a clean contained surface under red fluorescent light and allowed to explore and roam. Exploration activity levels were rated as normal, low, or high. Gait was assessed by observing toe scrunching, delay in foot lifts, high stance, and back arching behavior during walking. Any abnormalities as stated above were recorded. Abdominal pain-like features such as back arching, writhing, and twitching were analyzed and marked as present or absent according to the criteria outlined by the University of Michigan Unit of Laboratory Animal Medicine (ULAM) [65]. Puffing of the fur and lack of grooming was marked as pronounced, if the animal had a rough hair coat with fur facing outwards. At the end of behavioral assessment, grimace and porphyrin staining was analyzed under white, fluorescent light. To analyze grimace, each animal was held by an experimenter and frontal photos of each animal were taken. Photos were scored for orbital tightening, nose/cheek flattening, ear changes and whisker changes based on the criteria outlined by ULAM with "0" being not present, "1" being present and "2" being pronounced [65]. Porphyrin staining and pigment on hair coats are also indicators of lack of grooming which may be an indicator of pain and or stress [65]. The coverage and amount porphyrin staining around the top and sides of neck, head, cheeks, back, left side of flank, right eye, left eye, both eyes, and shoulders were scored by two observers with "0" being no porphyrin staining to "4" being intense brown staining, then summed for the total score. Porphyrin scores in all regions were summed and the maximum score is 40, with higher scores indicating a lack of grooming, an indirect indicator of animal distress.

Motion Segment Processing

At the conclusion of the safety study, the animals were humanely euthanized via CO_2 inhalation as the primary euthanasia method and bilateral pneumothorax as the secondary euthanasia method. The L5–L6 motion segments from each animal were resected and cleaned using a saw, bone cutters and a scalpel. Then, each motion segment was fixed in 3 mL of 4 % paraformaldehyde (PFA) (Sigma Aldrich, St. Louis, MO, USA, 441244-1KG) in 12-well plates at room temperature for 24 hours with constant agitation (180 rpm) on an orbital shaker. After fixation, the samples were washed 3 × 15 minutes with 1X PBS and decalcified in 3 mL of Immunocal (Fisher Scientific, Waltham, MA, USA, NC9044643) for 18 hours at room temperature under constant agitation (180 rpm) on an orbital shaker. Decalcified samples were washed 3 × 15 minutes with 1X PBS, then cryopreserved in 30 % wt/v sucrose solution prepared in 1X PBS for 24 hours at 4 °C. Finally, the sections were cryoembedded in Optimal Cutting Temperature Compound (Scigen 4586) and subsequently sectioned in the sagittal plane at 15 and 40 μm thicknesses.

Histological Processing

Hematoxylin and eosin (H&E) is a widely used colorimetric staining method to identify different tissues in the disc and assess the degree of degeneration [66]. Hema-

toxylin stains cell nuclei dark purple while eosin stains the extracellular matrix and cytoplasm pink. An acid alcohol solution was prepared by combining 70 % Ethanol (Decon Labs, King of Prussia, PA, USA, 2701) and 1 % Hydrochloric acid (11.9 M, Sigma Aldrich, H1758) in ultrapure MilliQ water (MQH_2O) for the differentiation process to remove background staining. A sodium acetate solution was prepared by dissolving 1 % wt/v sodium acetate (Sigma Aldrich, W302406) in MQH_2O and pH was adjusted between 8.5 to 9.0 using HCl or NaOH. The sodium acetate solution was used for the bluing step in H&E staining process, where it will convert the initial red color of the hematoxylin nuclei stain to blue.

To begin the staining process, sequentially, 15 μm thick motion segment sections on glass slides were post-fixed in 4 % PFA for 10 minutes, washed 3 $\times$ 5 minutes in 1X PBS and 1 minute in MQH_2O, then stained in Ehrlich's Hematoxylin (EMS, Hatfield, PA, USA, 26753-01) for 3 minutes, washed 4 $\times$ 30 seconds in MQH_2O, dipped 12 times repeatedly in acid alcohol solution, washed 2 $\times$ 1 minute in MQH_2O, blued in sodium acetate solution for 2 minutes, washed 3 $\times$ 1 minute in MQH_2O, dehydrated with 70 % Ethanol for 1 minute, counterstained with Eosin Y solution (EMS, 26762-01) for 20 seconds, rinsed in 70 % Ethanol twice for 2 seconds, and dehydrated in 95 % and 100 % Ethanol for 2 $\times$ 2 minutes each. Finally, the sections were dehydrated in xylene (Sigma Aldrich, 214736) for 1 minute and mounted using Permount mounting medium (Fisher Scientific, SP15-100).

Brightfield images of the H&E-stained motion segments were captured using an Axiocam 305 microscope, 0.63X camera adapter, and 5X objective (Carl Zeiss Microscopy), then stitched on ImageJ (Version 1.54, FIJI) [67]. H&E images study were scored by three blinded observers according to the standardized histopathology scoring system for rat discs [62,66].

Efficacy Study

The overarching goal of the second study was to test the efficacy of Pyr and Vcr at alleviating pain in our previously established disc injury rat model of disc-associated LBP. This model was selected because it exhibits similar characteristics to human degenerated disc pathology such as extracellular matrix breakdown, hypocellularity, inflammation, aberrant nerve sprouting and axial hypersensitivity, thereby increasing potential translation of treatment efficacy to the human disease state [62].

Forty-eight female Sprague Dawley rats (16-week-old) were included in the efficacy study and randomly assigned to four groups of equal size (n = 12): Sham, Injured + PBS, Injured + Pyr, and Injured + Vcr (Fig. 1**b**). The animals from the same group in the efficacy study were co-housed in pairs within the same cage. Sample sizes were calculated to ensure sufficient power (β = 0.8) and 95 % confidence (α = 0.05) to detect a 50 % recovery in grip strength in treated animals compared to injured animals assuming a standard deviation that was 11 % of the mean. Two animals from the Sham group were excluded from grip strength and gait analysis on week 13 because of animal's weight loss greater than 10 %. At the study conclusion, one animal from Injured + Pyr group was excluded from the study due to unrelated surgery complications, and one animal from Injured + Vcr group was excluded from the study due to mis-puncture confirmed by disc volume and histological analysis.

Surgical Procedure and Disc Injury

The surgical procedure and approach to expose the L5–L6 disc were performed as described above. Once the L5–L6 disc was located, the disc injury procedure was performed as described in our previous work [62]. Briefly, the L5–L6 disc was punctured bilaterally with a strong point dissecting needle (Roboz, Gaithersburg, MD, USA, RS-6066) set to 3 mm depth, then swept back and forth along a 90° arc six times in the transverse plane [62]. A continuous subcuticular suture closure pattern was used to close the abdominal wall and skin incision. All animals were injected subcutaneously with Buprenorphine SR (0.75 mg/kg) and monitored 1 hour post-operatively and then every 12 hours for 3 days after surgery for signs of pain or distress and wound closure. Animals were allowed to heal for two weeks after surgery before beginning behavioral data collection.

Pain Assessments

Grip Strength Axial Hypersensitivity. To assess whether the animals display signs of axial LBP, a grip strength assay was performed. The grip strength assay is particularly useful in studying evoked pain-like behavior in rodents as lower strengths are suggestive of axial hypersensitivity associated with disc degeneration [62,68,69]. Prior to data collection, animals were acclimated to the grip hold and grip strength apparatus (Columbus Instruments, Columbus, OH, USA, 1027SR) for six days and at least two minutes per day. For data collection, the animals were positioned to allow the forepaw to naturally grip onto a metal wire mesh, and then the animal was gently stretched in the caudal direction by the tail until its grip was released [62]. The outputs on a force sensor attached to the wire mesh show the maximum grip strength per trial. Three readings were collected with a 1-minute break between trials to increase the reliability of the measures. The average max force (N) of the three trials was calculated and reported as grip strength threshold. According to the Weber-Fechner law [70], the relationship between stimulus and perception is logarithmic. Hence, all grip strength thresholds were log base 2 transformed to achieve normality and then normalized to the animal's own baseline value. Grip strength was assessed every 2 weeks after disc injury surgery (weeks 2, 4, 6, 8, 10) and every week after intradiscal injection surgery (weeks 13, 14,

15) (Fig. 1**b**). The number of animals per group was split equally into two sets and the grip assay was performed by two blinded female experimenters with each experimenter performing the assay on one set of animals throughout the study.

Open Field Test. Non-stimulus dependent assays reduce subjectivity in detecting pain-like behavior in rodents. Movement-evoked pain-like and anxiety-like behavior can be observed without experimenter manipulation through the animal's exploration in a novel environment, such as an open field, within a short time frame [71]. The open field test was conducted by placing each animal in a custom-built acrylic 2' × 2' × 2' (L × W × H) black opaque arena [72]. The animals were not acclimated to the arena prior to data collection to maintain the novelty effect [73]. Three separate open field test recording sessions were conducted in week 0 (baseline), week 10 and 15 (Fig. 1**b)** in a dark room illuminated with red fluorescent lighting and draped with diffuser fabric over the arenas to avoid glares and shadows on the arena floor. Thirty-minute video recordings of individual animals in each arena were recorded using an overhead low-light camera (ALPCAM, Amazon, Seatle, WA, USA). At the end of each test, the arena was cleaned with Ethanol-soaked paper towels before placing the next animal in the arena. The middle 20 minutes of the videos were analyzed using EthoVision (Version 16, Noldus, Leesburg, VA, USA) for total distance traveled, maximum velocity, acceleration, mean turn angle and the total duration of unsupported rearing, supported reading, grooming, and frequency in the center zone (20 cm × 20 cm).

Gait Analysis. Gait analysis is another surrogate measure of stimulus-independent pain-like behavior and can be used to assess the progression of pain and disability longitudinally [74]. A number of techniques have been developed to analyze rodent gait, but The Gait Analysis Instrumentation and Technology Optimized for Rodents (GAITOR) Suite is an open source code for rodent gait analysis [72]. The GAITOR suite consists of a custom-built acrylic arena with a black acrylic back and lid, three transparent acrylic sides, and a transparent floor with a 45° mounted mirror underneath [72]. The detailed arena and lighting setup of the system are described elsewhere [72,75]. Eight animals from each group were acclimated twice for 10 minutes in the arena, 5 days apart, and once for 30 minutes two weeks before disc injury surgery. Gait trial collection was performed on weeks 3, 5, 7, 9, 13 and 14 post-disc injury (Fig. 1**b**). During the day of the experiment, the animals were removed from their home cage, weighed, and placed on one end of the arena. Video clips of the animal walking across the arena were recorded using a high-speed camera (Phantom, Wayne, NJ, USA, Miro C321) and Phantom Camera Control Version 3.8 software (Phantom) using the following settings: 1280 × 720 resolution, 500 fps sample rate and 300 μs exposure. Each animal remained in the arena for up to 30 minutes or until a minimum of nine successful trials containing at least two complete gait cycles were obtained. At the end of each test, the arena was cleaned with water soaked KimWipes before placing the next animal in the arena. Videos were analyzed to determine spatiotemporal gait patterns using a video processing software called Automated Gait Analysis Through Hues and Areas (AGATHA) [72,76]. Temporal symmetry, spatial symmetry, and duty factor imbalance are velocity-independent measurements. Duty factor, stride length, and step width are velocity-dependent measurements, and thus were plotted against trial velocity for each week and group.

Computed Tomography and Disc Volume Analysis

μCT scans of the L5–L6 disc were collected at weeks 0, 10, and 15 using a Quantum GX2 μCT Imaging System. Briefly, the rat was anesthetized and placed in the scanner in the supine position. Animals were scanned for 2 minutes with 90 kV power, 88 μA tube current, 45 mm field of view (FOV), 90 mm voxel size, and a Cu 0.06 + Al 0.5 x-ray filter. Following collection, data were exported as a VOX file and transferred to Analyze 14.0 (Analyze Direct, Overland Park, KS, USA) for disc volume analysis. Disc volume quantification was performed using a method previously developed in our lab [77]. In short, a 700 Hounsfield units (HU) threshold was used for each scan to identify bony objects [78,79]. The bony objects were then locked to prevent modification, and the L5–L6 disc space was colored in with the manual drawing tool beginning with the ventral most slice. Coronal smoothing and propagating objects, two semi-automatic tools, were used after the drawing was complete to reduce variability between each slice. When completed, drawings were saved as an object map. Disc volume was quantified using built-in software to analyze the object maps, and the volume of the object corresponding to the disc space was recorded.

Intervention Surgery and Intradiscal Axonal Dieback Compound Injection

On week 11 post-injury, the intradiscal injection procedure was performed and the injured animals were injected with 2.5 μL of either 1X PBS, 1 mM Pyr or 500 nM Vcr exactly as described above in the safety study. For the Sham animals, the L5–L6 disc was visualized and then abdominal cavity was closed. All animals were injected subcutaneously with Buprenorphine SR (0.75 mg/kg) and monitored post-operatively for 1 hour and every 12 hours for 3 days after surgery for signs of pain or distress and wound closure. Animals were allowed to heal for two weeks after surgery before beginning behavioral data collection.

Post-Processing of Tissue Samples

Necropsy and Tissue Processing: At the conclusion of the efficacy study (week 15), the animals were humanely

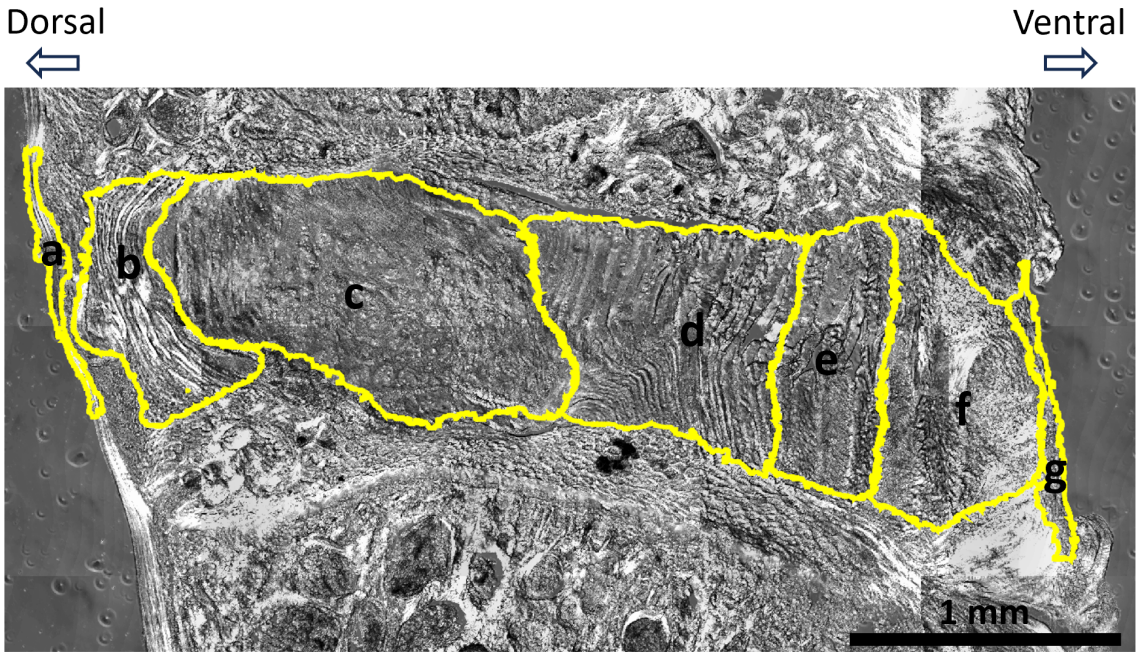

Fig. 2. Regions of the L5–L6 disc. Brightfield images of L5–L6 motion segments were used to outline the (a) dorsal ligament, (b) dorsal annulus fibrosis, (c) nucleus pulposus, (d) inner 2/3 of ventral annulus fibrosus, (e) outer 1/3 of ventral annulus fibrosus, (f) granulation tissue, and (g) ventral ligament. Scale bar = 1 mm.

euthanized via CO_2 inhalation as the primary euthanasia method and bilateral pneumothorax as the secondary euthanasia method. The L5–L6 motion segments from each animal were resected and processed as described above in the safety study to yield 15 and 40 μm sections of the motion segment. Additionally, the right T13 to L2 DRGs were removed, placed into individual microcentrifuge tubes, immediately flash frozen in liquid nitrogen, and stored in the –80 °C freezer until further analysis.

Histological Processing: Three 15 μm thick L5–L6 motion segment sections from each animal were processed and stained with H&E as outlined above in the safety study. Brightfield images of the H&E-stained motion segments were captured using an Axioscan 7 slide scanner with a 5X objective (Carl Zeiss Microscopy, Oberkochen, Germany). H&E images were randomly ordered and scored by three blinded observers according to the standardized histopathology scoring system for rat discs [62,66].

Immunohistochemistry (IHC): To understand the effects of axonal dieback compounds to nerves in the discs, the nerve fibers in the discs were stained using immunohistochemical methods to specifically locate the nerves and calculate the area of nerve fibers in the disc. Based on previous evidence showing positive protein gene product 9.5 (PGP9.5) and peptidergic C-fiber marker, calcitonin gene-related peptide (CGRP) staining in the disc [23,62,80,81], these two markers were selected to identify different nerve fiber types in the disc. Three 40 μm thick L5–L6 motion segment sections with 40 μm intervals were post-fixed in 4 % PFA for 15 minutes at room temperature, then washed 2 × 5 minutes in 1X PBS and 1 × 5 minutes in 1X PBST (1X PBS + 0.1 % Tween20). Immediately after washes, in a humidified slide tray, the sections were blocked and permeabilized with blocking buffer (1X PBS + 0.3 % TritonX-100 + 3 % goat serum) for 1 hour at room temperature, then incubated with blocking buffer containing primary antibodies: 1:100 mouse-derived anti-CGRP (Abcam, Cambridge, UK, ab81887) and 1:100 rabbit-derived anti-PGP9.5 (Abcam, ab108896) for 14 hours at 4 °C. After primary antibody incubation, the slides were washed 3 × 15 minutes in 1X PBST followed by incubation with secondary antibodies: 1:500 goat-derived anti-mouse AlexaFluor 488 (Abcam, ab150117) and 1:100 goat-derived anti-rabbit AlexaFluor555 (Abcam, ab150086) for 2 hours at room temperature in a humidified slide tray. Finally, the sections were washed 3 × 15 minutes in 1X PBST, stained for 10 minutes with 4′,6-diamidino-2-phenylindole (DAPI) diluted 1:1000 in 1X PBS, washed 3 × 5 minutes in 1X PBS and mounted with ProLong Gold Antifade Mountant (Thermo Fisher, Waltham, MA, USA, P36930) and glass coverslips (Globe Scientific, Mahwah, NJ, USA, 1415-15). Tiled Z-stack fluorescent and transmitted light images of the entire section (3 sections/motion segment) were acquired using a Zeiss LSM 800 Confocal Microscope (Carl Zeiss Microscopy) with a 10X objective and tiling features. The respective excitation and detection wavelengths (nm): DAPI (405, 400–450), AF488 (488, 450–564), and AF555 (561, 564–700) were used to acquire these images.

Z-stack projections of the motion segment images were created using ZENBlue (Version 2.5, Carl Zeiss Mi-

Table 1. List of genes and sequences for quantitative polymerase chain reaction.

Gene name	Target	Forward sequence	Reverse sequence
ACTB	β-Actin	GCTATGAGCTGCCTGACGGT	GTTTCATGGATGCCACAGGA
TRPV1	Transient receptor potential vanilloid 1	CTCGGTTCTGGAGGTGATCG	AGTCGGTTCAAGGGTTCCAC
TRPA1	Transient receptor potential ankyrin 1	GCAGCATTTTCAGGTGCCAA	CGCTGTCCAGGCACATCTTA
Piezo2	Piezo type mechanosensitive ion channel component 2	CCTGTGGCAAAACATGACCG	GACCTTGGCATGGCTGTAGA
Scn9a	Voltage-gated sodium channel Nav1.7	TCTCCGACTAAGCCATCAGG	GCGCTAGAAAAAGGGACAGG
CHRNA3	Cholinergic receptor nicotinic alpha 3 subunit	CGCCTGTTCCAGTACCTGTT	TTCTCTGCAGGAACACGCAT
PTGER2	Receptor for prostaglandin E2	GACCACCTCATTCTCCTGGC	CTCGGAGGTCCCACTTTTCC
Bdkrb1	Bradykinin receptor b1	CAACAGCTGCTTGAACCCAC	CTGGGTATCTTTGTGGGCTGT
NGF	Nerve growth factor	AGGCTTTGCCAAGGACG	CCAGTGGGCTTCAGGGA

Table 2. Number of DRGs with detectable and non-detectable readings per group for qPCR (number of animals (detect/non-detect)).

Gene	Sham	Injured + PBS	Injured + Pyr	Injured + Vcr	cDNA dilution
TRPV1	12/0	12/0	11/0	12/0	1:10
TRPA1	12/0	12/0	11/0	12/0	1:20
Piezo2	12/0	12/0	11/0	12/0	1:10
Scn9a	12/0	11/1	11/0	12/0	1:10
CHRNA3	12/0	10/2	10/1	12/0	1:10
PTGER2	12/0	12/0	12/0	11/1	1:20
Bdkrb1	12/0	12/0	11/0	10/2	1:10
NGF	11/1	12/0	11/0	12/0	1:20

DRGs, dorsal root ganglia; qPCR, quantitative polymerase chain reaction; PBS, phosphate-buffered saline; Pyr, pyridoxine; Vcr, vincristine; cDNA, complementary DNA.

croscopy) and saved as .czi files. The .czi files were imported into QuPath v 0.4.4 [82] for region-specific quantification and analysis. For each section, the annotations for dorsal ligament, dorsal AF, NP, inner 2/3 of the ventral AF, outer 1/3 of the ventral AF, granulation tissue, and ventral ligament regions were manually outlined using the wand tool (Fig. 2). Once the regions were drawn, the "Pixel Classifier" tool was used to set a threshold above 30 and 40 to identify PGP9.5 and CGRP positive area staining, respectively. A minimum pixel area of 60 μm^2 was set to minimize the inclusion of background fluorescence and noise. The percentage of positively stained protein gene product (PGP) and CGRP areas in each region were calculated and compared between groups. Usable sections without excessive non-specific background staining from 11 Sham, 12 Injured + PBS, 8 Injured + Pyr, and 10 Injured + Vcr animals were analyzed for PGP staining, while sections from 11 Sham, 12 Injured + PBS, 10 Injured + Pyr, and 10 Injured + Vcr animals were analyzed for CGRP staining (**Supplemental Fig. 1**).

Hypocellular tissue is a common trait of degenerated discs due to cell apoptosis [83]. To quantify disc cellularity, the "Cell detection" tool in QuPath was used to outline each nucleus in the DAPI images. The number of cell detections in each region divided over the region area were reported as nuclei/mm^2 and compared between groups.

DRG Quantitative Polymerase Chain Reaction (qPCR) Analysis

DRGs are a cluster of neuronal cell bodies connecting the peripheral nervous system to the central nervous system. Injury can alter gene transcription in the DRG which contributes to nervous system plasticity [84]. Gene expression levels of ion channels, nociceptors, inflammatory mediators, and neuronal injury were examined to determine changes in transcription of DRGs post-injury and post-treatment. Quantitative polymerase chain reaction (qPCR) was used to assess gene expression in right T13, L1 and L2 DRGs combined per animal. These DRG levels were selected since L1 and L2 DRG neurons primarily innervate the L5–L6 disc in rats [85,86]. Prior to all qPCR experiments, all equipment was cleaned with a surface decontaminant RNAse AWAY (Thermo Fisher, 21-402-178). DRG tissue was uniformly homogenized using sterile homogenizer probes (USA Scientific, Ocala, FL, USA, 1415-5390) and spring scissors (Fine Science Tools, Foster City, CA, USA, 15024-10). Cells were lysed using TRI reagent (Sigma Aldrich, T2924) and 1-Bromo-3-chloropropane (Sigma Aldrich, B9673) prior to phase separation. A high salt solution with 2-Propanol (Sigma Aldrich, I9516) was used to precipitate ribonucleic acid (RNA) before purification with RNAsecure resuspension solution (Thermo Fisher, AM7010). RNA was synthesized into complementary DNA (cDNA) using iScript cDNA Synthesis Kit (Bio-Rad, Hercules, CA, USA, 1708890) ac-

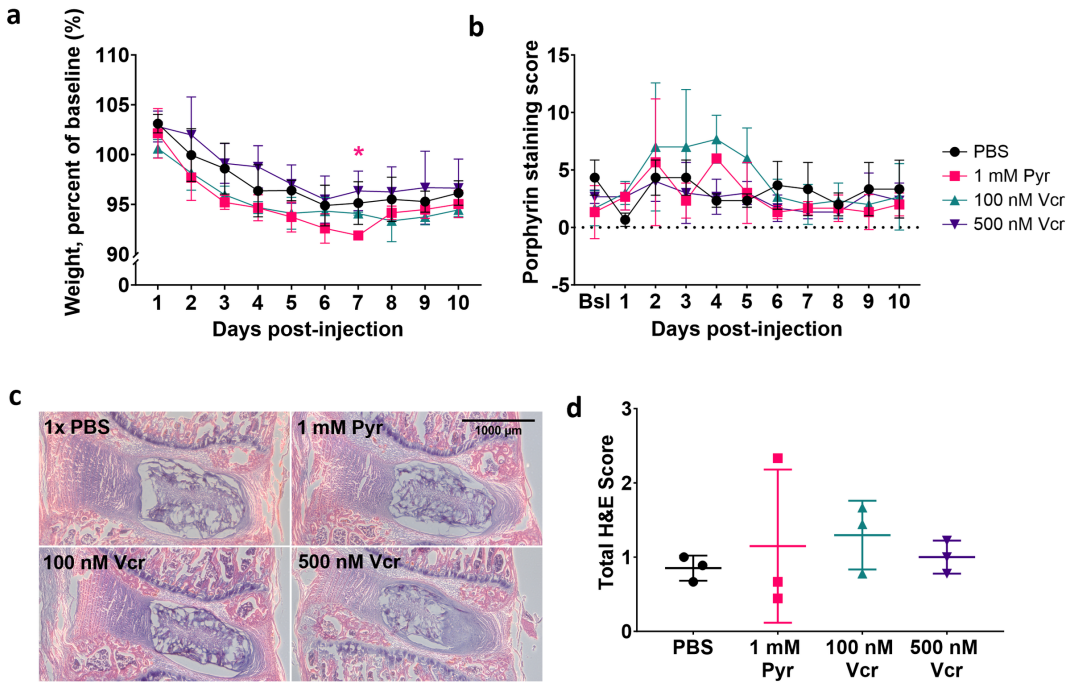

Fig. 3. Pyridoxine and vincristine intradiscal injection did not affect animals general health and showed normal disc morphology. (**a**) Animal weight significantly decreased over time, as expected, but did not differ between groups. (**b**) Porphyrin staining score was low indicating low animal distress, which was not significant between groups. (**c**) Brightfield images did not show signs of disc degeneration. Scale bar = 1000 μm. (**d**) Total H&E score of motion segments was not significantly different between groups (n = 3 per group). Bsl, baseline. $^{*}p < 0.05$.

cording to manufacturer's protocol for a target of 1 μg/μL of cDNA per animal. qPCR primer pairs (Table 1) were designed using National Institutes of Health (NIH) Primer-Blast tool. All primer pairs were validated and determined to have primer efficiencies between 90–110 %. For each primer pair, cDNA samples from each animal were run in duplicate at 1:10 to 1:20 cDNA dilution in nuclease-free water (VWR, Randor, PA, USA, 82007-336). Experiments were run on an Azure Biosystems (Azure Cielo, Azure Biosystems, Dublin, CA, USA) machine using SYBR green reagents (Bio-Rad, ge-0794) with a maximum of 40 polymerase chain reaction (PCR) cycles. Relative gene expression for each group was calculated using the $2^{-\Delta\Delta C}{}_{q}$ method by using the average of *ACTB* (β-Actin) levels as the normalization gene per animal. If results were non-detected, a Cq value of 40 was assigned for the respective gene [87]. The number of detected and non-detected animals per gene for each group and cDNA dilution are displayed in Table 2.

Statistical Analysis

Normality of data was assessed using Shapiro-Wilks test. Normally distributed data were analyzed using one-way Analysis of Variance (ANOVA) when comparing more than two groups or 2-way ANOVA when comparing groups across time. For non-normal data, Kruskal-Wallis test was applied to compare groups within each week and Friedman test to compare between weeks or days within each group. Table 3 summarizes the data analyzed with their corresponding normality and tests. Alpha value was set to 0.05 and all asterisk symbols reported on graphs represent $p <$ 0.05. Generated plots show the mean and standard deviation error bars. Gait data show the mean and 95 % confidence intervals. For nerve fiber staining and DRG transcription level correlation analysis with grip strength, the data were not normally distributed, so nonparametric Spearman correlation coefficients were calculated.

Results

Safety Study

Intradiscal Injection of Axonal Dieback Compounds are Safe

No health concerns or signs of animal distress were observed up to 10 days after intradiscal injection of either Pyr (1 mM), Vcr (100 nM, 500 nM) or vehicle (PBS). After surgery, all animals exhibited a temporary tendency for mild pica behavior, which resolved within two days. This behavior is a common side effect of buprenorphine-induced nausea, and thus, not concerning [88]. All animals had significant decrease in weight over time ($p < 0.0001$), but the animal weights were not significantly different between groups (Fig. 3**a**). The animal weights decreased similarly in all groups at no more than 9 % weight loss from baseline,

Table 3. List of data and methods used for statistical analysis.

Data	Normality	Statistical analysis method
Safety study (n = 3/group)		
Animal weights (raw data, normalized)	Yes	2-way ANOVA with repeated measures (Tukey's post-hoc)
Total porphyrin score	No	Kruskal-Wallis test (Dunn's post-hoc)
H&E score	Yes	One-way ANOVA (Tukey's post-hoc)
Efficacy study (n = 11–12/group)		
Animal weights (% of baseline)	No	Kruskal-Wallis test (Dunn's post-hoc)
Grip strength (log_2) (normalized)	Yes	2-way ANOVA with repeated measures (Tukey's post-hoc)
Comparing grip strength pre-treat and post-treat (log_2) (normalized)	Yes	Multiple paired *t*-tests
Disc volume (raw data, normalized)	Yes	2-way ANOVA with repeated measures (Tukey's post-hoc)
H&E score	No	Kruskal-Wallis test (Dunn's post-hoc)
Open field test (n = 11–12/group)		
Distance travelled	Yes	2-way ANOVA with repeated measures (Tukey's post-hoc)
In center zone (frequency)	Yes	2-way ANOVA with repeated measure (Tukey's post-hoc)
Grooming (duration)	No	Kruskal-Wallis test (Dunn's post-hoc)
Turn angle	Yes	2-way ANOVA with repeated measure (Tukey's post-hoc)
Supported rearing (duration)	No	Kruskal-Wallis test (Dunn's post-hoc)
Unsupported rearing (duration)	No	Kruskal-Wallis test (Dunn's post-hoc)
Gait measurements (n = 10/group)		
Step width, stride length, duty factor, duty factor imbalance, temporal symmetry, spatial symmetry	Normality verified via density plot	Linear mixed effects model, where week and groups were treated as fixed effects and animals as random effects
Immunostaining (n = 8–11/group)		
PGP area (%) in DL	Yes	One-way ANOVA
PGP area (%) in all regions (except DL) and combined disc regions	No	Kruskal-Wallis test (Dunn's post-hoc)
CGRP area (%) in all regions and combined disc regions	No	Kruskal-Wallis test (Dunn's post-hoc)
DAPI cell counts in all regions	No	Kruskal-Wallis test (Dunn's post-hoc)
DAPI cell counts in combined disc regions	Yes	One-way ANOVA
DRG PCR (n = 11–12/group)		
Fold change: *TRPV1*	Yes	One-way ANOVA (Sidak's post-hoc)
Fold change: *TRPA1*, *Piezo2*, *CHRNA3*, *PTGER2*, *Bdkrb1*, *Scn9a*	No	Kruskal-Wallis (Dunn's post-hoc)
Correlations	No	Spearman

ANOVA, Analysis of Variance; H&E, hematoxylin and eosin; PGP, protein gene product; DL, dorsal ligament; CGRP, calcitonin gene-related peptide; DAPI, 4′,6-diamidino-2-phenylindole; PCR, polymerase chain reaction.

demonstrating that the general health of the animals was not affected by the intradiscal injection of axonal dieback compounds. On day 7, the percentage of weight loss from baseline was significantly greater in the 1 mM Pyr group compared to the 100 nM Vcr group, but the 1 mM Pyr animals quickly gained weight afterward injection and reached similar weights to other groups from day 8 onwards (Fig. 3**a**). All animals displayed normal activity levels throughout the time course. No changes in rat grimace were observed throughout the study. For gait, two out of three rats in the 500 nM Vcr group had visibly higher stance while walking by day 7 post-injection. Pain-like features such as back arching, writhing, and twitching were absent except for two out of the three rats in the 500 nM Vcr group that had mild to moderate back arching by day 6 post-injection. These observations lasted until day 10 (end of study) but did not affect the animal's activity level. The average total porphyrin staining score had significant changes over time but not between groups (Fig. 3**b**). Histological staining with H&E shows signs of healthy discs without any tissue disruption or loss of shape and cellularity (Fig. 3**c,d**). H&E scores did not differ significantly between groups suggesting that intradiscal injection of PBS, Pyr or Vcr did not affect disc matrix or lead to disc degeneration in the 10-day time course (Fig. 3**c**). The results from the safety study verified the safety of injecting Pyr (1 mM) and Vcr (100, 500 nM) locally into L5–L6 discs.

Efficacy Study

Axonal Dieback Compounds did not Alter Disc Degeneration

After determining the safety of axonal dieback compounds in the disc, an efficacy study using the highest doses of Pyr and Vcr as axonal dieback compounds (1 mM Pyr, 500 nM Vcr) was conducted to test the effectiveness of the compound in alleviating pain-like behavior. Animal weights increased over time and did not differ significantly between groups during the efficacy study, which

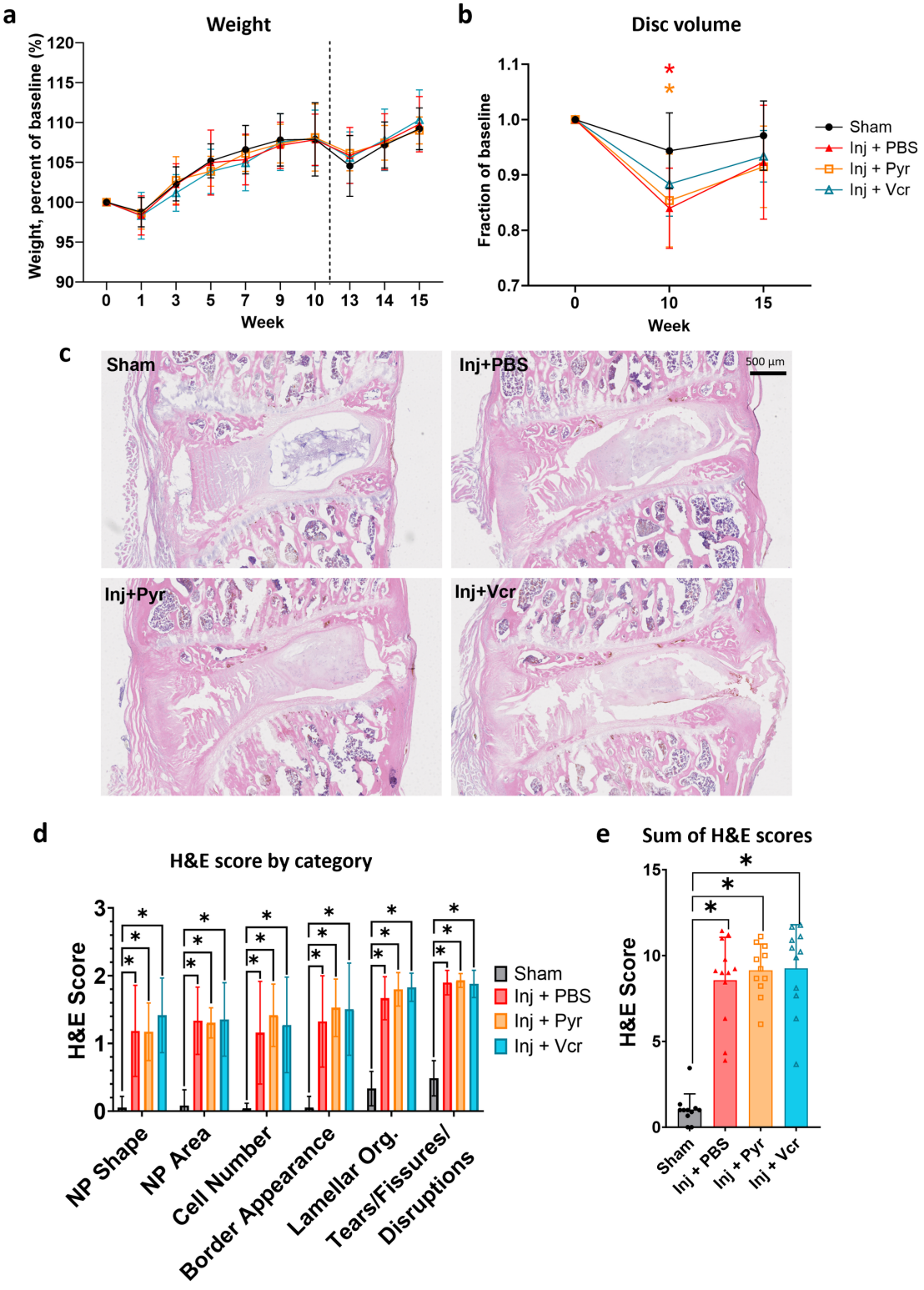

Fig. 4. Disc scrape injury induced disc degeneration and axonal dieback compounds did not alter disc degeneration. (**a**) Overall, animal weights increased over time and did not differ between groups at any time point. Small declines in weight were observed in all groups post-surgically. (**b**) Injured animals disc volume as a fraction of baseline decreased and was significantly lower compared to Sham at week 10; however, significance was lost by week 15. (**c**) Brightfield images of H&E-stained L5–L6 motion segments showed disrupted AF tissue, and loss of NP shape and cellularity in all injured and treated discs. Scale bar = 500 μm. (**d**) H&E scores in injured and treated groups were significantly higher than Sham for all categories. (**e**) Sum of H&E scores across all categories were significantly higher in injured and treated groups compared to Sham. $^{*}p < 0.05$. Inj, Injured; AF, annulus fibrosus; NP, nucleus pulposus; org., organization.

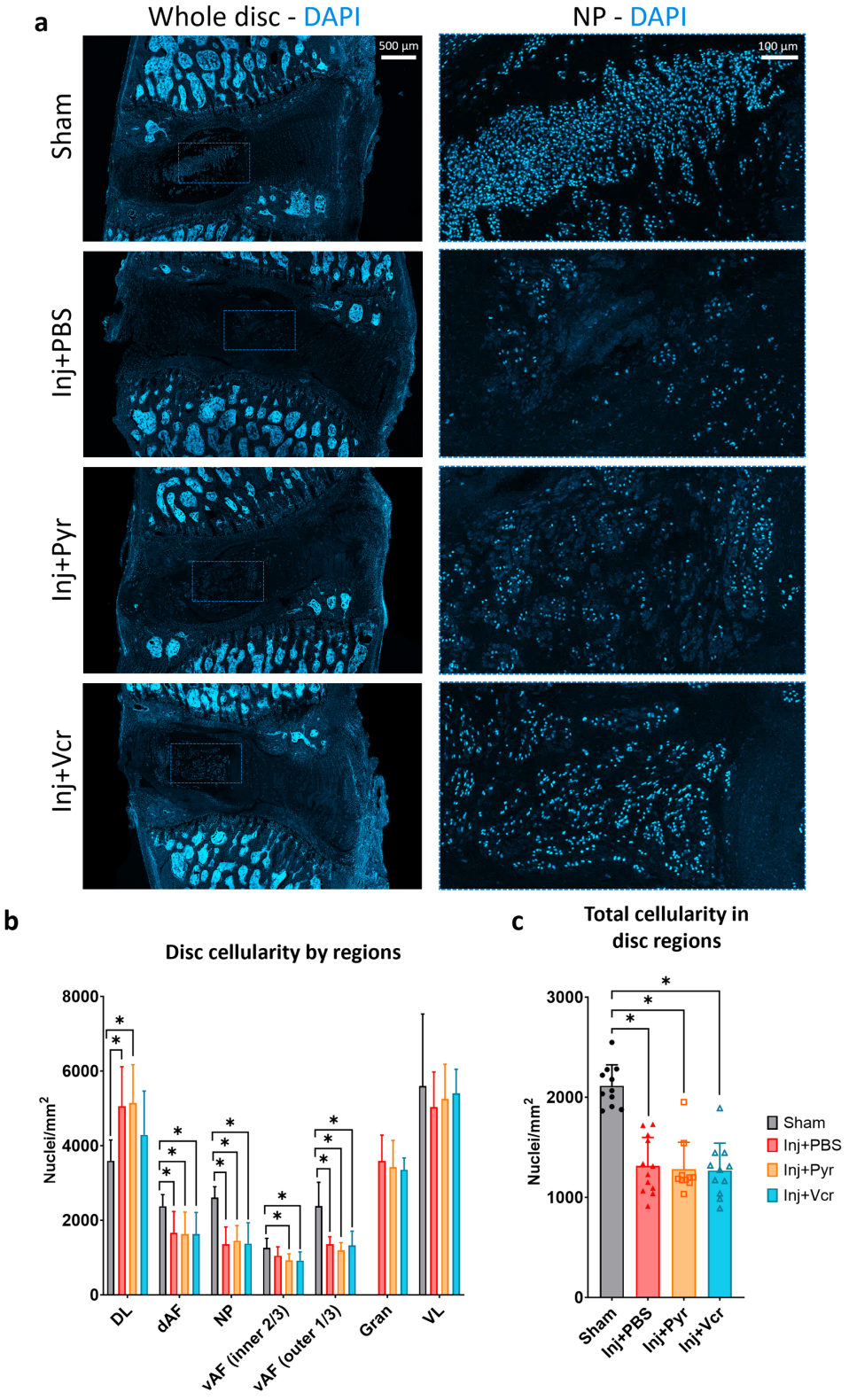

Fig. 5. DAPI staining in L5–L6 disc reduced after disc scrape injury but was not aggravated by treatment. (**a**) Fluorescent images of DAPI staining showed reduced cell number and cell clustering in NP of injured discs. Scale bar = 500 μm or 100 μm. (**b**) Cell nucleus counts normalized to region area were significantly lower in all injured and treated discs compared to Sham. (**c**) Total cell nucleus counts in the disc were significantly lower in all injured groups compared to Sham. No differences in cell nucleus count between injured groups suggested that axonal dieback compounds did not induce additional cell death. $^{*}p < 0.05$. DAPI, 4′,6-diamidino-2-phenylindole; DL, dorsal ligament; dAF, dorsal annulus fibrosus; vAF, ventral annulus fibrosus; Gran, granulation tissue; VL, ventral ligament.

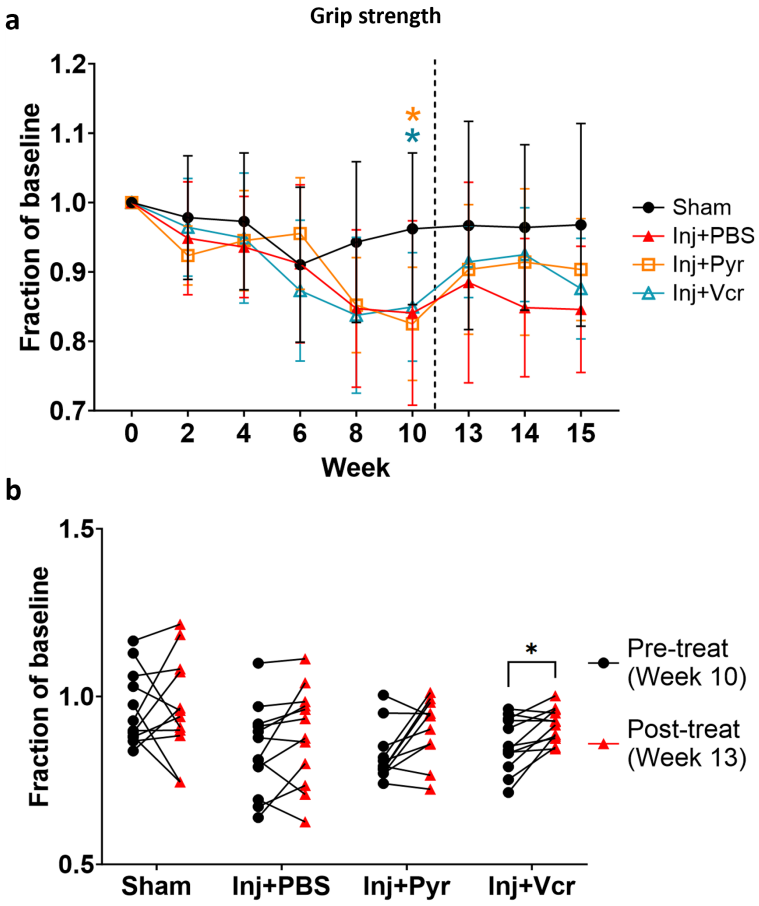

Fig. 6. Axial hypersensitivity measured by grip strength assay was evident after disc injury and was partially alleviated after intervention with axonal dieback compounds. (**a**) Grip strength normalized to baseline decreased in all injured groups over time and Injured + Pyr and Injured + Vcr groups became significantly reduced compared to Sham by week 10. After intervention surgery, Injured + Pyr and Injured + Vcr groups had partial recovery towards baseline but did not reach significance compared to Injured + PBS group, whereas Injured + PBS group remained decreased although not significant compared to Sham. Statistical analysis was performed using repeated measures 2-way ANOVA excluding baseline data (week 0). (**b**) Change in normalized grip strength values before (black circle) and after (red triangle) intervention showed increasing trends in most of the animals in Injured + Pyr and Injured + Vcr groups as compared to Sham and Injured + PBS. Normalized grip strength in Injured + Vcr group significantly increased from week 10 (pre-treatment) to week 13 (2 weeks post-treatment). $^{*}p < 0.05$. ANOVA, Analysis of Variance.

again proves the safety of the injection procedure and axonal dieback compounds tested (Fig. 4**a**).

Disc volume analysis showed the progression of disc degeneration as a result of the 6-scrape disc injury with a 16 %, 14.6 % and 12.3 % loss of disc volume from baseline in PBS, Pyr and Vcr injured groups in week 10, respectively. There was a significant and substantial reduction in disc volume at week 10 compared to baseline in all injured groups ($p = 0.0001$ for PBS, $p = 0.0004$ for Pyr, $p = 0.0001$ for Vcr). At week 10, the Injured + PBS ($p = 0.0042$) and Injured + Pyr groups ($p = 0.0212$) experienced significant loss of disc volume compared to Sham, while Injured + Vcr group approached significance ($p = 0.135$) (Fig. 4**b**). Between weeks 10 and 15, the average disc volume in all injured groups increased from 84.0–88.4 % to 91.5–93.4 %. Disc volume for Sham group also increased closer to baseline from 94.4 % in week 10 to 97.1 % in week 15 which is consistent with our previous findings [62]. No significant differences in disc volume were detected between groups in week 15 (Fig. 4**b**).

The L5–L6 discs of the Sham animals were healthy with no signs of degeneration while there are obvious signs of degeneration in the injured discs, including AF tears and disruption and changes in NP morphology (Fig. 4**c**). H&E scores used to assess the degree of disc degeneration revealed that the discs of the injured group were significantly more degenerated than the discs in Sham animals in all individual categories as well as in the total score ($p = 0.0002$–0.002) (Fig. 4**d,e**). No significant differences were observed between the injured groups indicating that the injection of Pyr and Vcr did not impact or alter disc degeneration (**Supplemental Fig. 2**). Concurrent with disc degen-

eration, the cells in the disc undergo apoptosis and the disc becomes hypocellular [89]. Therefore, it is not surprising that the disc cellularity quantified from DAPI staining in the disc in all injured groups was significantly lower compared to Sham ($p < 0.0001$) (Fig. 5**b,c**). All injured groups have similar levels of disc cellularity with no significant losses in the Injured + Pyr and Injured + Vcr groups compared to the Injured + PBS group suggesting that there was no additional cell death due to Pyr and Vcr injection in the discs.

Axial Hypersensitivity did not Significantly Recover after Axonal Dieback Compound Injection in a Female Rodent Disc-Associated LBP Model

In the efficacy study, injured animals in Injured + Pyr ($p = 0.0131$) and Injured + Vcr groups ($p = 0.0445$) had significantly reduced normalized grip strength thresholds while Injured + PBS group ($p = 0.0993$) approached significance compared to Sham (Fig. 6**a**). After intradiscal injection of compounds, Pyr- and Vcr-treated groups had increased normalized grip strength, recovering towards baseline values that were maintained up until week 15 (4 weeks post-injection); however, values did not rise to a level of significance compared to the Injured + PBS (Fig. 6**a**). When comparing the individual normalized grip strength values immediately pre- and post-intervention from weeks 10 to 13, respectively, more animals in Injured + Pyr and Injured + Vcr groups had increasing grip strength values compared to Sham and Injured + PBS, but only the Injured + Vcr group values reached a level of significance ($p = 0.031$) (Fig. 6**b**). As expected, the Injured + PBS group had no effect on axial hypersensitivity as the normalized grip strength values remained significantly lower compared to Sham at both weeks 14 and 15 (2 and 3 weeks post-injection) (Fig. 6**a**).

Disc Injury and Axonal Dieback Compound Injection did not Result in Movement-Evoked Pain-Like Behaviors in a Female Rodent Disc-Associated LBP Model

In the open field test, the total distance travelled, frequency in center zone, and duration spent rearing both supported and unsupported significantly decreased over time for all groups ($p < 0.0001$) (Fig. 7**a,b,e,f**), while the mean turn angle significantly increased over weeks in all groups ($p < 0.0001$) (Fig. 7**d**). Time spent grooming did not change significantly over time or between groups (Fig. 7**c**). All the activities measured in open field test did not differ significantly between groups (Fig. 7). These data demonstrate that neither the disc injury or intradiscal injection with PBS or axonal dieback compounds influenced the animals' exploratory behavior in the open field test. However, as animals were increasingly exposed in the arena and as the animals age across weeks, there is a significant effect on some of the animals' exploratory behavior over time.

Disc Injury or Axonal Dieback Compound Injections did not Affect Velocity-Dependent Spatiotemporal Gait Patterns in a Female Rodent Disc-Associated LBP Model

The average walking velocity for all animals was between 58 to 66 cm/second over time and did not differ significantly between groups or over time. Step width and stride length are velocity-dependent gait measures that assess the animal's spatial gait patterns, while duty factor is a velocity-dependent gait measure that describes the gait temporal sequence. The linear model results showed that all animals in all groups displayed normal trends in velocity-dependent gait patterns, with step width and duty factor decreasing with velocity, and stride length increasing with velocity in both fore and hind limbs (Figs. 8,9). Statistical analysis between groups showed that hindlimb step width, hindlimb stride length and both right and left hindlimb duty factor were not significantly altered between groups over all timepoints (Fig. 8). These findings were consistent in forelimb gait analysis (Fig. 9). Therefore, these data suggest that disc injury and PBS or axonal dieback compound injections did not produce movement-evoked pain-like behaviors or impact spatiotemporal gait up to 9 weeks post-injury and 3 weeks post-intervention.

Disc Injury or Axonal Dieback Compound Injections did not Affect Symmetrical Gait Patterns in a Female Rodent Disc-Associated LBP Model

The symmetry of a gait pattern describes the distance in space or time between the left and right limbs, such that a left limb should land at halfway (50 %) between two right limb foot strikes. Hence, spatial symmetry describes the spacing of left and right footprints, where temporal symmetry describes the timing of left and right foot strikes. Hind duty factor imbalance describes the amount of time spent on the left and right limbs, where 0 % indicates that an equal amount of time is spent on both limbs. Our analysis revealed that animals walked with balanced stance times and a temporally and spatially symmetric gait across all groups and weeks (Fig. 10**a,c,e**). These findings were consistent in forelimb gait analysis (Fig. 10**b,d,f**). Overall, these results suggest that the effects of disc injury surgery and intervention with axonal dieback compounds were mild and did not induce movement-evoked pain-like behaviors or gait impairment.

PGP and CGRP Staining in the Disc Increased after Disc Injury

PGP9.5 and CGRP areas in the L5–L6 discs of Sham animals were minimal to none (Figs. 11,12, and Table 4). Nerve fibers positively stained with PGP and CGRP lining the needle entry track were visually prominent in the ventral AF in all injured discs (Figs. 11,12). PGP9.5 and CGRP immunostaining in the inner two thirds of the ventral AF increased significantly in the Injured + PBS compared to Sham which indicates nerve infiltration after disc injury ($p = 0.0008$, 0.0194) (Figs. 11**b**,12**b**). The Injured

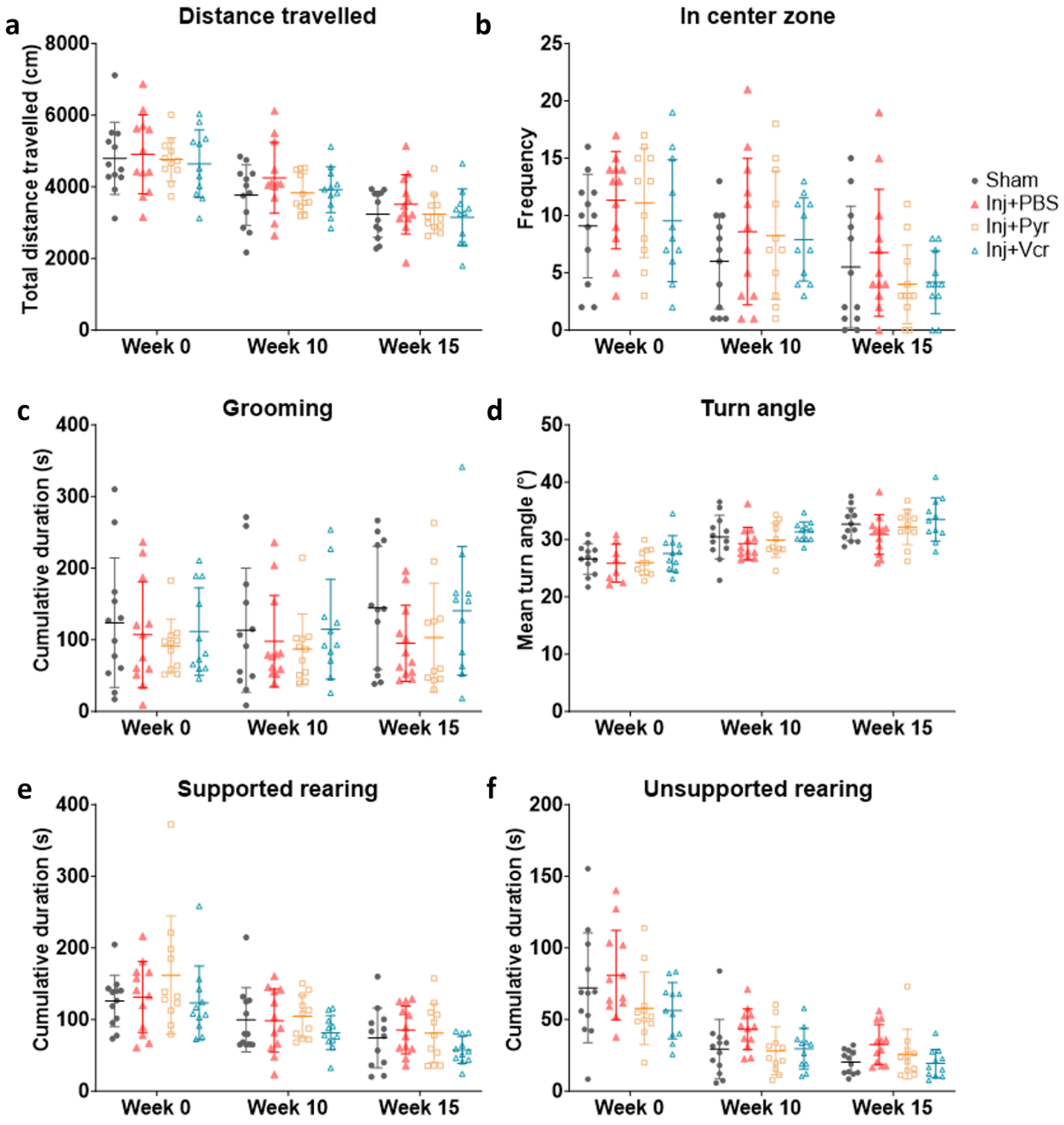

Fig. 7. Open field test behavior analysis did not reveal any significant differences between groups. No significant differences were detected in (**a**) total distance travelled, (**b**) frequency in the center zone, (**c**) grooming, (**d**) turn angle, (**e**) supported rearing, and (**f**) unsupported rearing between Sham, Injured + PBS, Injured + Pyr and Injured + Vcr groups in all weeks.

+ PBS group had increased total PGP9.5 area to 2.732 % from 0.095 % in Sham but did not reach significance compared to Sham (Fig. 11**c** and Table 4). The total CGRP area in the Injured + PBS group was 1.654 %, which was significantly higher compared to Sham at 0.493 % (p = 0.0014) (Fig. 12**c** and Table 4). The data confirm the presence of nerve fibers including peptidergic C-fiber nociceptors innervating injury-induced degenerated discs.

PGP and CGRP Staining in the Disc Reduced after Pyr Injection, but not after Vcr Injection

Pyr injection at 1 mM successfully induced axonal dieback within the disc as evidenced by decreased PGP9.5 in regions of the disc from the dorsal AF to the ventral ligament (Fig. 11**b**) and decreased CGRP in dorsal AF (Fig. 12**b**), although it did not reach significance compared to Injured + PBS. Only in the granulation tissue, Pyr injection significantly reduced PGP9.5 and CGRP areas compared to Injured + PBS (p = 0.0135, 0.0169) and Injured + Vcr groups (p = 0.0043, 0.0212) (Figs. 11**b**,12**b**). Overall, in

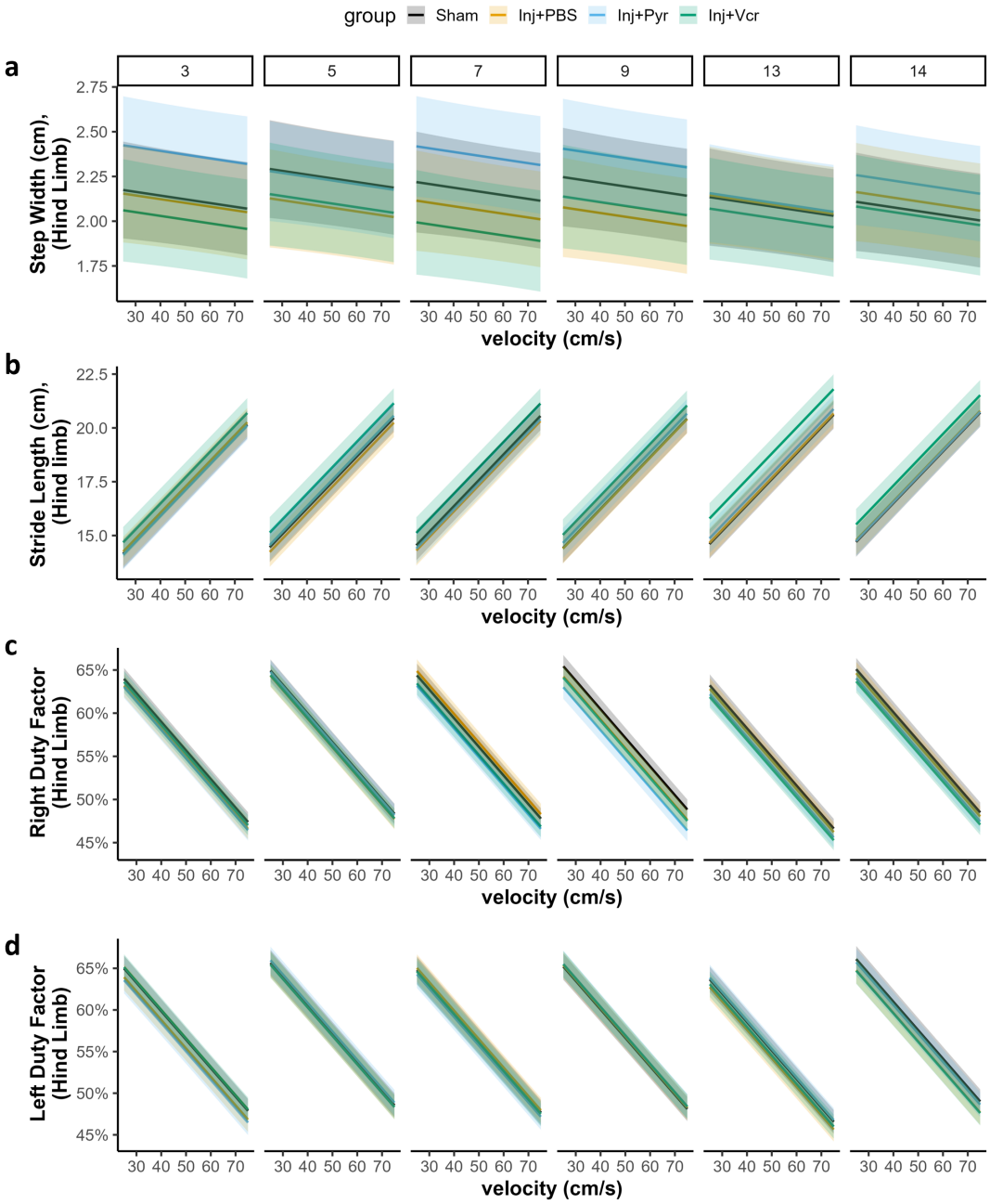

Fig. 8. Velocity-dependent spatiotemporal gait analysis of the hindlimbs identified normal gait patterns in all groups over time. (**a**) Step width, (**b**) stride length, (**c**) right hindlimb duty factor, and (**d**) left hindlimb duty factor. The number in boxes at the top represents the weeks for the graphs in each graph column. Lines are linear mixed effect models and bands represent the 95 % confidence intervals.

the disc, the percentage of total PGP9.5 and CGRP areas in the combined disc regions were reduced to 1.198 % and 0.861 % in Injured + Pyr group compared to 2.732 % and 1.654 % in Injured + PBS but failed to reach significance compared to Injured + PBS group (Figs. 11**c**,12**c** and Table 4). A bolus injection of 1 mM Pyr significantly reduced nerves in some parts of the disc.

On the other hand, Vcr injection did not have the same effect as Pyr. The PGP9.5 and CGRP areas in the granulation tissue, ligaments, and disc regions of the Injured + Vcr group were similar to the Injured + PBS group (Figs. 11**b**,12**b**). Further, the total PGP9.5 area in the disc was 3.117 % comparable to 2.732 % in Injured + PBS group and the total CGRP area in the disc was 1.463 % significantly higher compared to Sham (p = 0.0034) and similar to 1.654 % in Injured + PBS group indicating that the aberrant nerves were retained after Vcr injection (Figs. 11**c**,12**c** and Table 4). A bolus injection of Vcr at 500 nM did not induce axonal dieback within the disc.

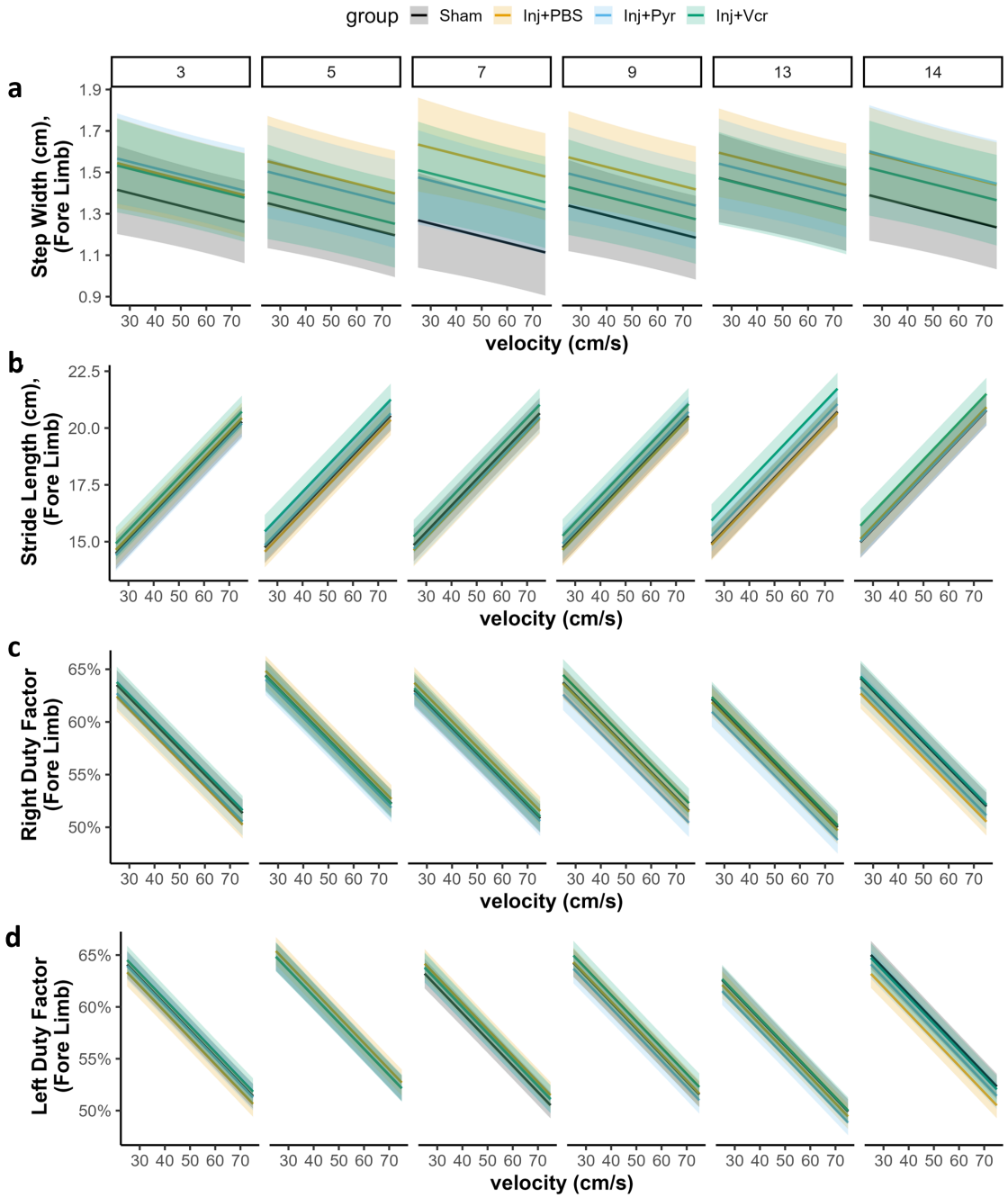

Fig. 9. Velocity-dependent spatiotemporal gait analysis of the forelimbs identified normal gait patterns in all groups over time. (**a**) Step width, (**b**) stride length, (**c**) right forelimb duty factor, and (**d**) left forelimb duty factor. The number in boxes at the top represents the weeks for the graphs in each graph column. Lines are linear mixed effect models and bands represent the 95 % confidence intervals.

Nerve Fiber Presence and Peptidergic C-Fiber Markers in the Discs are Correlated with Axial Hypersensitivity

In correlation to the grip strength thresholds, total PGP staining in the disc was significantly negatively correlated to normalized grip strength (r = –0.3395, p = 0.0299) (Fig. 13**a**). Total CGRP staining in the disc was also significantly negatively correlated to normalized grip strength (r = –0.3298, p = 0.0308) (Fig. 13**b**). This indicates that increased innervation of nerve fibers and small peptidergic C-fibers in the disc are correlated to lower grip strength values and increased axial hypersensitivity.

Disc Injury Induced Significant Increase in DRG Gene Expression Levels of Pro-Inflammatory Mediator, *Bdkrb1* and Ion Channels of Mechanosensation and Nociception, *Piezo2* and *Scn9a*

Ion channel gene expression in DRGs such as *TRPV1*, transient receptor potential ankyrin 1 (*TRPA1*), piezo type mechanosensitive ion channel component 2 (*Piezo2*) and

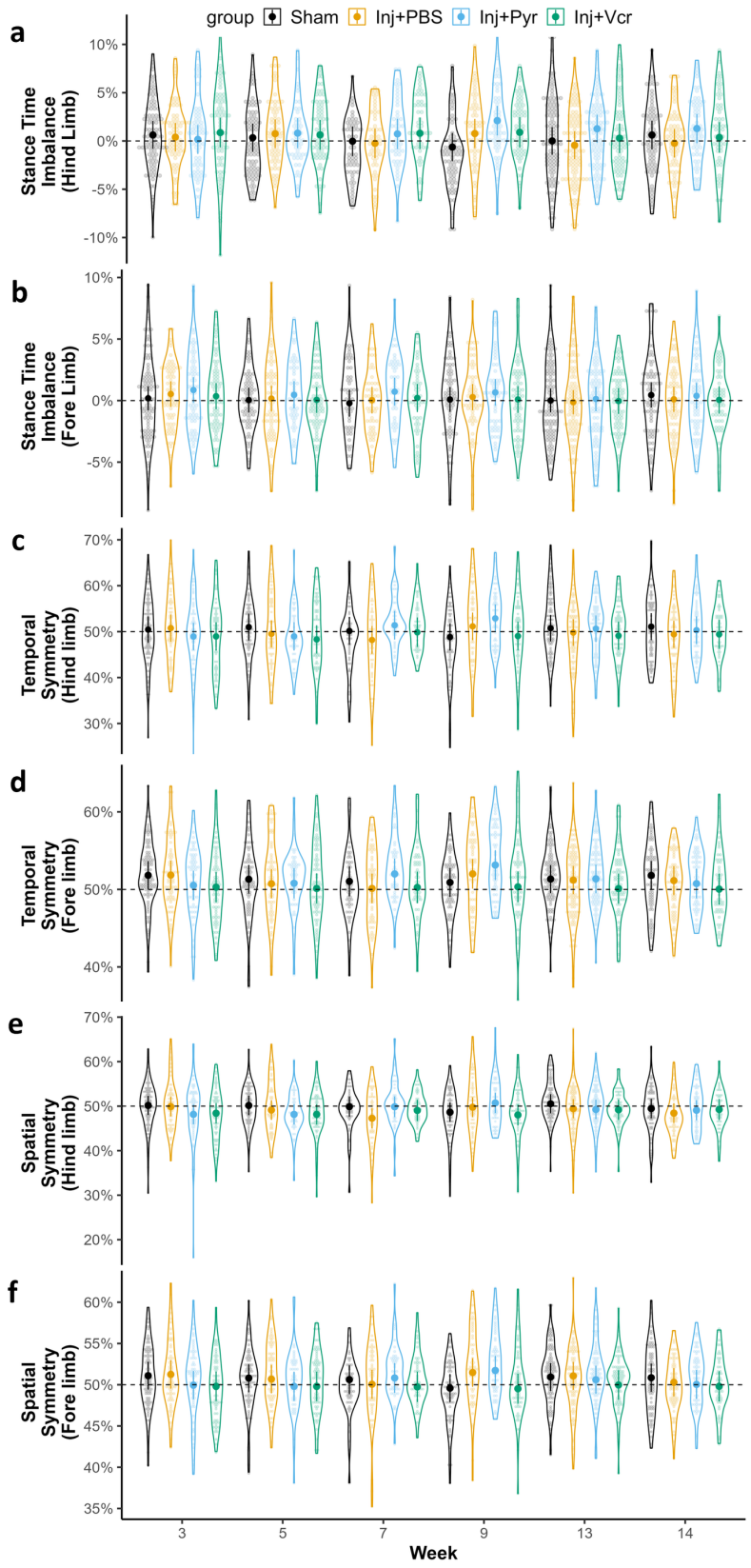

Fig. 10. Non-velocity-dependent spatiotemporal gait analysis exhibited symmetrical gait patterns and sequence in all groups over time. Stance time imbalance for (**a**) hindlimb and (**b**) forelimb; temporal symmetry of the (**c**) hindlimb and (**d**) forelimb; and spatial symmetry of the (**e**) hindlimb and (**f**) forelimb. Data were distributed around the dashed lines representing absence of duty factor imbalance (0 %) and presence of symmetric gait (50 %). Violin plots show the data distribution while the large marker and error bars show the mean and 95 % confidence interval.

Table 4. Mean and standard deviation of total PGP- and CGRP-stained area in the combined NP, AF, and granulation tissue regions of L5–L6 disc sections.

Group	Total PGP9.5 area (%)	Total CGRP area (%)
Sham	0.0947 (0.719)	0.493 (0.242)
Injured + PBS	2.732 (2.540)	1.654 (1.218)
Injured + Pyr	1.198 (0.390)	0.861 (0.545)
Injured + Vcr	3.117 (2.566)	1.463 (0.835)

NP, nucleus pulposus; AF, annulus fibrosus; PGP9.5, protein gene product 9.5.

voltage-gated sodium channel Nav1.7 (*Scn9a*) was upregulated in Injured + PBS group but only *Piezo2* ($p = 0.0264$) and *Snc9a* ($p = 0.0053$) reached significance, compared to Sham (Fig. 14**a**). Gene expression of silent nociceptor marker, cholinergic receptor nicotinic alpha 3 subunit (*CHRNA3*), increased in Injured + PBS group but did not significantly differ from Sham (Fig. 14**b**). Inflammatory mediators-related genes such as bradykinin receptor b1 (*Bdkrb1*), receptor for prostaglandin E2 (*PTGER2*) and nerve growth factor (*NGF*) were upregulated in Injured + PBS group compared to Sham but only *Bdkrb1* reached significance compared to Sham ($p = 0.0015$) (Fig. 14**c**). These data suggest that disc scape injury in the L5–L6 disc may be related to increased gene expression levels of pro-inflammatory *Bdkrb1* and ion channels such as *Piezo2* and *Scn9a* in the T13 to L2 DRGs innervating the disc.

Since CGRP and PGP9.5 staining in the disc was increased in Injured + PBS discs compared to Sham (Figs. 11**c**,12**c**) and correlated significantly with grip strength (Figs. 13,14**d**), similar correlation analyses were also performed with DRG gene expression to further probe whether the relationship between disc injury and transcription in the DRG can be explained by increased innervation or pain behavior. Specifically, correlations of CGRP and PGP9.5 staining in the disc, DRG gene expression levels, and normalized grip strength values were examined to probe interactions between these factors. Fig. 14**d** delineates all significant correlations. DRG gene expression in pro-nociceptive ion channels, silent nociceptors and pro-inflammatory mediators is all significantly correlated with each other (Fig. 14**d**). Interestingly, none of the DRG genes investigated in this study were significantly positively correlated with disc PGP or CGRP staining (Fig. 14**d**). Additionally, neither of the DRG genes were significantly correlated with normalized grip strength values (Fig. 14**d**). These findings suggest that DRG gene transcription level is not directly correlated with nerve fiber presence in the disc or grip strength at week 15 post-injury.

Pyr Upregulated Gene Expression of DRG Nociceptive Ion Channels and Inflammatory Mediators Whereas Vcr Demonstrated a Downregulatory Effect

Differential gene expressions of ion channels and pro-inflammatory mediators in response to axonal dieback compounds were observed. Pyr significantly upregulated *TRPV1* ($p = 0.0161$), *TRPA1* ($p = 0.0176$), *Piezo2* ($p < 0.0001$), *Scn9a* ($p = 0.0006$) ion channel gene expression in DRGs compared to Sham (Fig. 14**a**). Further, pro-inflammatory mediator *Bdkrb1* ($p < 0.0001$), *PTGER2* ($p = 0.0076$) and *NGF* ($p = 0.0091$) gene expressions were also significantly upregulated in Injured + Pyr group compared to Sham (Fig. 14**c**). Pyr injection did not have significant effect on DRG gene expression analysis at four weeks post injection.

On the other hand, Vcr injection into the disc had the opposite effect. Vcr injection downregulated DRG gene expression level in all ion channels, silent nociceptor markers and pro-inflammatory mediators to similar levels found in Injured + PBS or restored levels similar to Sham group (Fig. 14**a–c**). *TRPV1* ($p = 0.0013$), *TRPA1* ($p = 0.0132$), *Piezo2* ($p = 0.0269$), *Scn9a* ($p < 0.0001$) ion channel gene expression in DRGs was significantly lower compared to elevated gene expression in Injured + Pyr group (Fig. 14**a**). The same trend was observed in silent nociceptor marker and pro-inflammatory mediator DRG gene expression where *CHRNA3* ($p = 0.0182$), *Bdkrb1* ($p < 0.0001$), *PTGER2* ($p = 0.0002$) and *NGF* ($p < 0.0001$) had significantly lower expression compared to Injured + Pyr group (Fig. 14**b,c**). In addition, DRG gene expressions were also lower compared to Injured + PBS group where significance was detected in *Scn9a* ($p = 0.0001$), *CHRNA3* ($p = 0.0004$), *Bdkrb1* ($p = 0.0004$), *PTGER2* ($p = 0.0088$) and *NGF* ($p = 0.0011$) gene expressions (Fig. 14**a–c**). Taken together, these data illustrate that Vcr injection locally into injured discs has down-regulatory effect on gene expression in DRGs four weeks post-injection, but upregulation after Pyr injection.

Discussion

Recent studies have explored denervation as an alternative treatment method to treat disc-associated LBP. Clinical studies involving denervation procedures such as radiofrequency electrodes [90–93], electrothermal energy [94], and methylene blue injection [40,41,95–100] to ablate nerve fibers innervating the discs have shown some promise of relieving pain short-term [96,97,99,101]. Nevertheless, the low quality of evidence and the mixed success rates in these studies [41,97,100–103] underscore the need for further research into disc denervation as a viable treatment method.

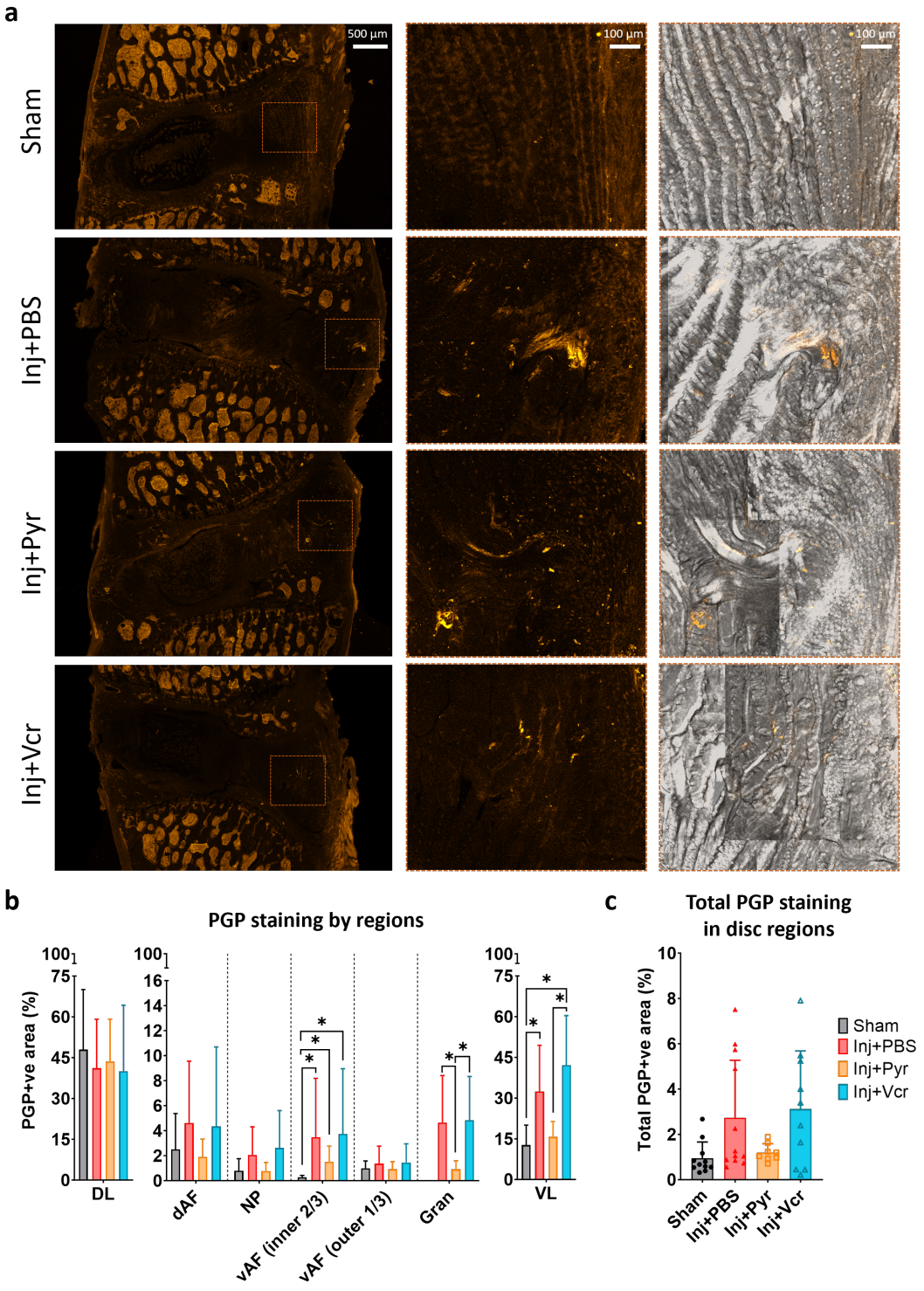

Fig. 11. Nerve fiber presence in the disc was increased with disc injury, while Pyr injection reduced nerve fiber presence in the disc, but Vcr did not. (**a**) Images of fluorescent PGP9.5 nerves in the ventral AF of all injured discs, nearby the needle puncture track. Boxes in image highlight the close-ups of regions of interest (ROIs) where positive PGP9.5 staining was observed in the ventral AF of injured discs. Scale bar = 500 μm or 100 μm. (**b**) PGP9.5 area increased within the disc and ventral ligament in Injured + PBS discs and PGP9.5 staining reduced after Pyr injection but not after Vcr injection. PGP9.5 area in the granulation tissue region was significantly lower after Pyr injection compared to Injured + PBS. (**c**) Total PGP9.5 area over NP and all AF regions in the disc were reduced after Pyr injection. Total PGP9.5 area did not reach significance in comparisons between groups. $^{*}p < 0.05$. DL, dorsal ligament; dAF, dorsal annulus fibrosus; NP, nucleus pulposus; vAF, ventral annulus fibrosus; Gran, granulation tissue; VL, ventral ligament; PGP9.5, protein gene product 9.5; PGP, protein gene product.

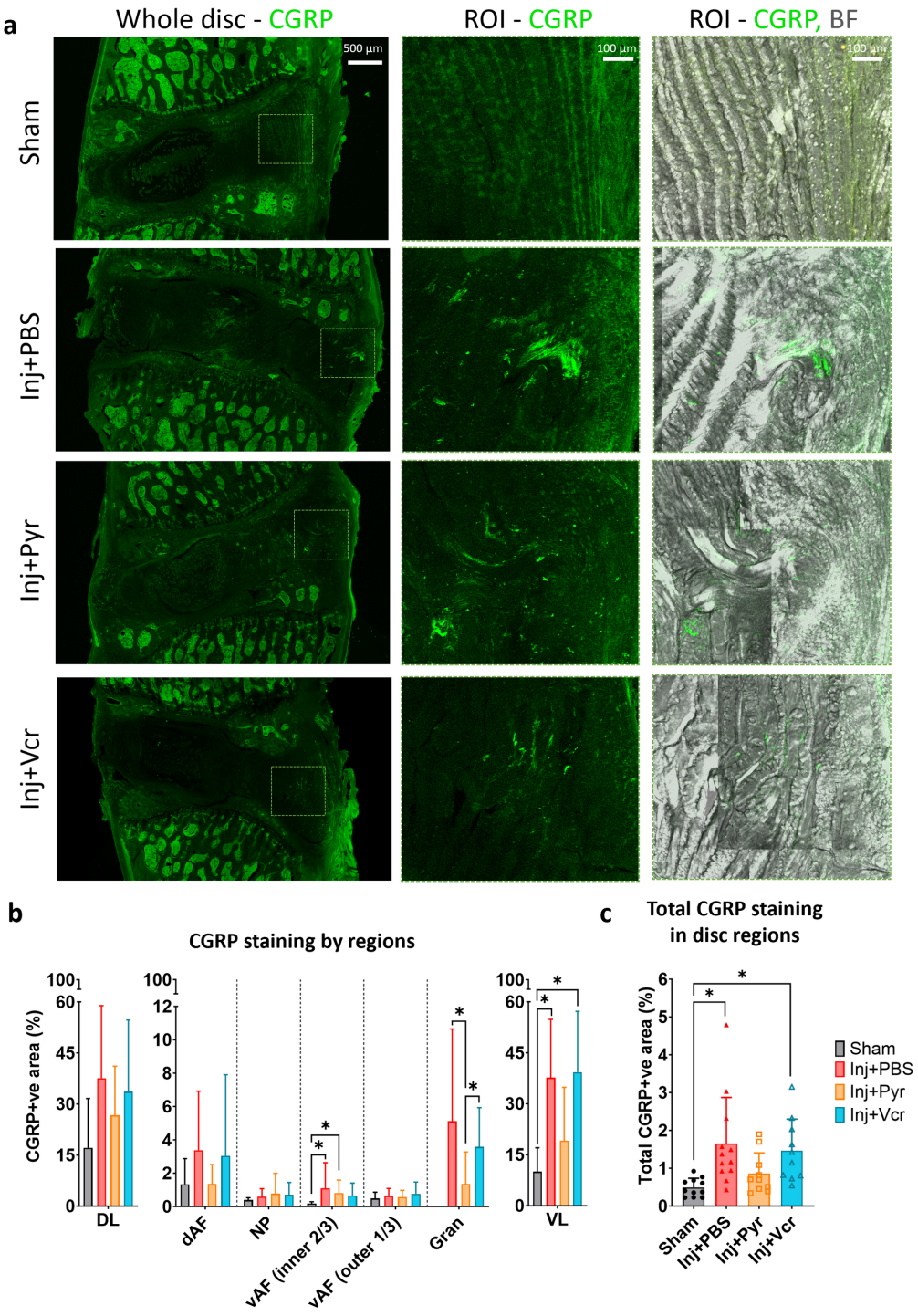

Fig. 12. C-fiber presence in the disc was increased in injured discs and decreased after Pyr injection but not Vcr injection. (**a**) Images of fluorescent CGRP nerves in the ventral AF of injured discs demonstrating innervation of injured discs after disc injury around the needle puncture track. Boxes in image highlight the close-ups of regions of interest (ROIs) where positive CGRP staining were observed in the ventral AF of injured discs. Scale bar = 500 μm or 100 μm. (**b**) CGRP area analysis in different regions of the disc showed significant reduction in CGRP staining in the granulation tissue after Pyr injection compared to Injured + PBS. (**c**) Total CGRP area over NP and all AF regions in the disc were significantly increased in Injured + PBS discs suggesting increased nociceptor innervation after disc injury. Similar to Injured + PBS group, Vcr-treated discs have significantly higher CGRP area in the disc which suggest that Vcr did not reduce nerve fiber in the disc after intervention. Pyr injection reduced CGRP staining but did not reach significance compared to Injured + PBS. $^{*}p < 0.05$. DL, dorsal ligament; dAF, dorsal annulus fibrosus; NP, nucleus pulposus; vAF, ventral annulus fibrosus; Gran, granulation tissue; VL, ventral ligament; CGRP, calcitonin gene-related peptide; BF, bright field; +VE, postive.

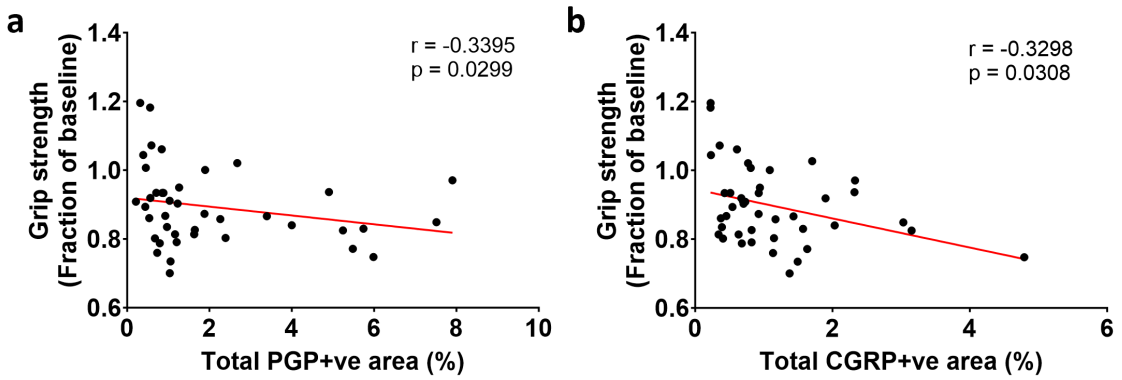

Fig. 13. Axial hypersensitivity is significantly correlated with the amount of nerve fiber present in the disc. (**a**) PGP9.5 area is significantly correlated with grip strength. (**b**) CGRP area is significantly correlated with grip strength.

The results of this study revealed that axonal dieback compounds Pyr and Vcr can be safely injected into degenerated discs to potentially treat disc-associated LBP. Animals that received the compounds in either healthy or degenerated discs in the safety study and efficacy study, respectively, exhibited normal activity, good overall health and did not suffer from any distress, severe pain, weight loss or disc degeneration which provide strong evidence that Pyr and Vcr are safe for intradiscal injection (Fig. 3). Pyr and Vcr did not induce acute disc damage in the safety study and did not alter or accelerate disc degeneration in the injured discs in the efficacy study (Figs. 3,4). Although the role of the nerves in the disc in the progression of disc degeneration is still unclear, it is important that the axonal dieback compounds do not cause further destabilization of degenerated discs during denervation treatment. Consistent with previous work, which demonstrated that the 1 mM Pyr and 500 nM Vcr are not cytotoxic to NP and AF cells *in vitro* [61], this study confirms the finding that Pyr and Vcr are cytocompatible, and they do not reduce cell number in the disc compared to the PBS-treated group (Fig. 5). Overall, these data suggest that Pyr and Vcr are safe to use for intradiscal injection into discs and do not cause disc degeneration or animal stress and pain. To identify LBP patients that may benefit from axonal dieback intradiscal injections, novel imaging technologies to diagnose "painful" discs with nerve ingrowth are needed. In the present-day, it is best to rule out other leading sources of pain and highly recommended that computed tomography (CT) or other imaging modalities such as magnetic resonance imaging (MRI) are used to verify that the discs are degenerated and thus may be symptomatic before intervening with dieback compounds.

This study is the first to investigate the safety and efficacy of Pyr and Vcr intradiscal injection and to explore the impact of disc denervation on pain-like behaviors in a rodent model of disc-associated LBP while examining for the presence of nerves in disc or lack thereof after denervation. Increased grip strength threshold, indicative of reduced axial hypersensitivity, was observed after intervention with Pyr and Vcr suggesting that the compounds partially alleviate pain-like behavior for up to four weeks after intervention (Fig. 6). However, the minor differences compared to Injured + PBS groups failed to reach significance suggesting that the effect of Pyr and Vcr was mild, and that statistical power was not sufficient to detect the differences. These findings of partial pain alleviation could also be related to the incomplete reduction of PGP9.5 and CGRP nerve fiber staining in disc compared to Sham levels in the Injured + Vcr animals (Figs. 11,12 and Table 4) and signs of DRG sensitization and inflammation in the Injured + Pyr group (Fig. 14).

The disc scrape injury successfully induced nerve ingrowth as indicated by the significantly increased area of both PGP and CGRP nerve fiber staining in Injured + PBS discs compared to control (Figs. 11,12). This result is consistent with our previous study describing the disc scrape injury [62]. The occurrence and colocalization of CGRP, C-fiber marker, with, PGP9.5, pan-neuronal marker in the Injured + PBS discs confirms that the nerve fibers are C-fiber type which concur with past immunohistochemical analyses of painful degenerated discs from human LBP patients have also found that nerve fibers innervating the disc are primarily C-fibers [20,23]. Pyr (1 mM) significantly reduced total CGRP area in the disc to an average 0.861 % compared to 1.654 % in Injured + PBS and 0.493 % in Sham, which marks a loss of small unmyelinated peptidergic C-fibers due to Pyr-induced denervation (Fig. 12 and Table 4). The observed significant correlation between total CGRP area and grip strength threshold provides evidence that small unmyelinated peptidergic C-fibers may play a key role in pain originating from the disc (Fig. 13). These results corroborate the findings of a great deal of previous work that identified the majority of nerves innervating degenerated rat [104,105] and human [23] discs are CGRP fibers which are related to the development of pain. This work shows that the reduction in CGRP-positive fibers could potentially reverse painful symptoms.

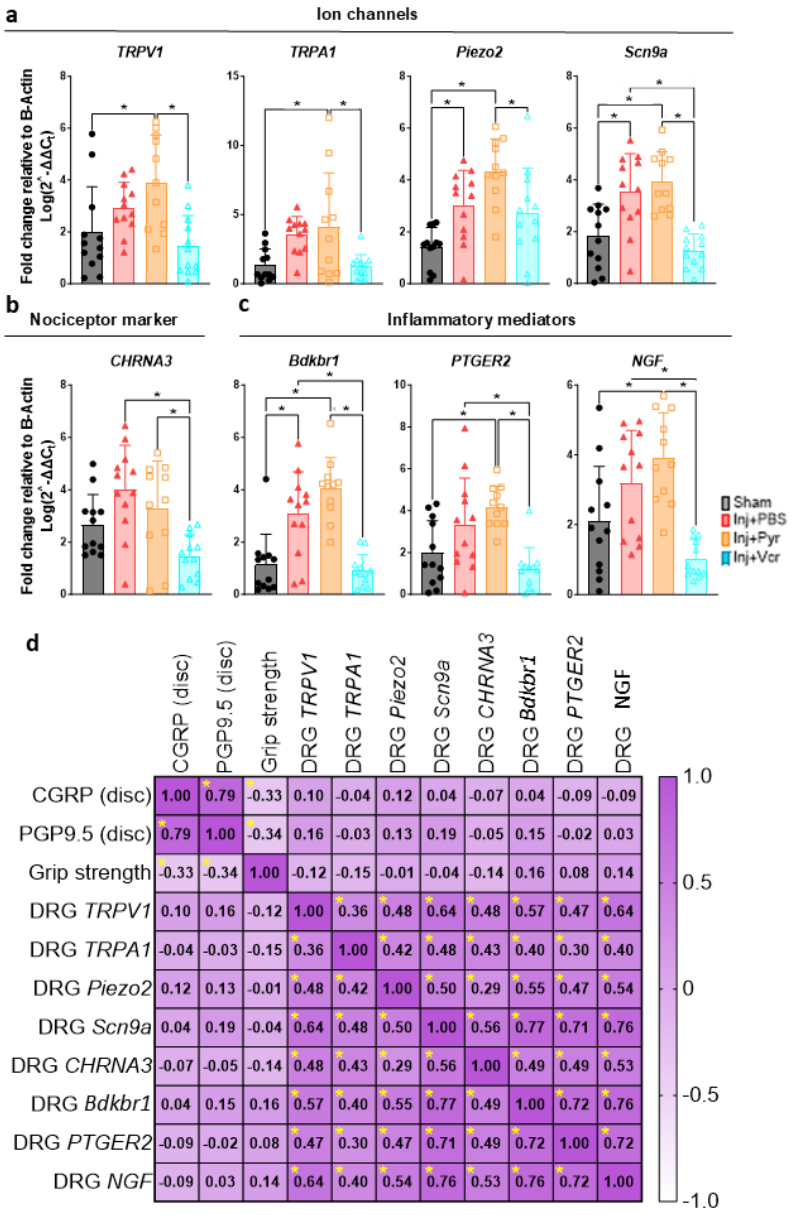

Fig. 14. DRG gene expression of pro-nociceptive ion channels, silent nociceptor marker, and pro-inflammatory mediators are not correlated with CGRP and PGP9.5 nerve fiber staining in the disc and pain-like behaviors at 15 weeks post-injury. Fold changes in DRG gene expression of (**a**) ion channels, (**b**) silent nociceptor marker, and (**c**) pro-inflammatory mediators between Sham, injured, and dieback treated animals show increased expression of ion channel markers *TRPV*, *TRPA1*, *Piezo2*, and *Scn9a* between Sham and Injured + Pyr animals. In addition, a significant increase in pro-inflammatory markers *Bdkrb1*, *PTGER2*, and *NGF* were observed between Sham and Injured + Pyr animals suggesting an increase in inflammation in DRGs from animals receiving pyridoxine treatment. $p \leq 0.05$, are indicated by black stars in (**a**), (**b**), and (**c**). (**d**) Correlation matrix showing correlations between DRG gene expression, PGP9.5 and CGRP nerve fiber staining in the disc, and normalized grip strength values shows significant correlations between DRG gene expression of ion channel markers *TRPV1*, *TRPA1*, and *Piezo2* with pro-inflammatory markers *Bdkrb1* and *PTGER2* between all animals. Significant correlations, $p \leq 0.05$, are indicated by yellow stars in the upper left corner within the matrix. DRGs, dorsal root ganglia; *TRPV1*, transient receptor potential vanilloid 1; *TRPA1*, transient receptor potential ankyrin 1; *Piezo2*, piezo type mechanosensitive ion channel component 2; *Scn9a*, voltage-gated sodium channel Nav1.7; *CHRNA3*, cholinergic receptor nicotinic alpha 3 subunit; *PTGER2*, receptor for prostaglandin E2; *Bdkrb1*, bradykinin receptor b1; *NGF*, nerve growth factor.

Surprisingly, no differences were found in PGP and CGRP staining in Vcr-treated discs even though the Injured + Vcr group displayed similar outcomes in partially relieving axial hypersensitivity as the Injured + Pyr group (Figs. 6,11,12). A possible explanation for this might be the different mechanism of Pyr and Vcr-induced axonal dieback. In our previous work, screening axonal dieback compounds in DRG explants *in vitro* with Pyr caused DRG axons to retract towards the soma and forming a bulbed end whereas Vcr caused blebbing and neurite fragmentation [61]. The positive staining of PGP9.5 and CGRP in Vcr-treated discs could be fragmented nerve debris from Vcr-induced nerve degeneration. Hence, these degenerated nerve fibers may be defunctionalized and no longer able to transmit signals. Therefore, nerve staining alone cannot be solely relied upon to draw definitive conclusions regarding the effectiveness of axonal dieback and pain alleviation. These results should be carefully interpreted, and future work can include markers of degenerated nerves for nerve immunohistochemistry (IHC) analysis.

Nerve ingrowth in injured discs can lead to neuronal sensitization and neuroinflammation in the DRG which is correlated to the induction and progression of disc-associated LBP [106]. *TRPV1*, *TRPA1*, and *Piezo2* are ion channels that have been shown to mediate neuronal sensitization in animal models of peripheral pain such as knee osteoarthritis [107–110]. Previous studies have found increased DRG macrophage activation and substance P production as early as three days after disc injury in rats [111]. Inflammatory mediators including *PTGER2* [112], *Bdkrb1* [113] and *NGF* [114] are commonly implicated in painful degenerative joint diseases. Herein, DRG gene expressions of pro-nociceptive ion channels, silent nociceptor markers, and pro-inflammatory mediators were examined to study the crosstalk between the disc and DRGs. In the disc-associated LBP model described herein, DRG *Piezo2*, *SCN9a*, *Bdkrb1* were significantly upregulated in Injured + PBS groups compared to Sham which suggests that disc injury may have a role in upregulating DRG sensitization and inflammation (Fig. 14**a,c**). Our data also support findings from a mouse model of disc-associated LBP that observed nerve growth factor, neuropeptide, proinflammatory mediator and ion channels were significantly upregulated in DRGs from animals with injured discs at 12 weeks post-injury [114]. Because DRG sensitization occurs in response to disc degeneration, and axonal dieback compounds only offer limited pain relief, studying DRG sensitization and neuroinflammation were examined in axonal dieback compound treated animals.

Our findings presented increased gene expression levels of pro-nociceptive ion channels, silent nociceptor marker and pro-inflammatory mediator in all injured groups at 15 weeks post-injury except for Injured + Vcr group, where DRG gene expression levels were reversed and significantly lower compared to Injured + PBS and Injured + Pyr groups (Fig. 14**a–c**). These data demonstrate that Pyr injection did not exacerbate DRG sensitization while Vcr injection may exhibit anti-nociceptive and anti-inflammatory properties in the connecting DRGs that lasts at least four weeks post-injury. The anti-nociceptive anti-inflammatory effects with Vcr have not been previously seen since Vcr is highly associated with chemotherapy-induced neuropathic pain and increased inflammatory cytokine production in the peripheral and central nervous system [115]. A key differentiator in the opposite effects shown here is the microdosing of Vcr locally in the disc versus a systemic prolonged exposure to the drug during chemotherapy. The data further suggest that Vcr and Pyr could have different mechanisms in alleviating axial hypersensitivity after intradiscal injection. The lack of full alleviation in axial hypersensitivity could be due to the presence of DRG inflammation and sensitization in Injured + Pyr group compared to Sham (Fig. 14**a,b**). Thus, it may be worth considering treatment at the DRG level to offer a more comprehensive pain relief when using Pyr as axonal dieback compound to treat disc-associated LBP. A limitation of this study is the end-point analysis for DRG gene expression analysis which limits our understanding of the temporal changes in DRG gene expression level after disc injury and axonal dieback compound injection.

It is also important to consider that the DRG contains various neuron types such as C-fibers, A-δ and A-β fibers. Using qPCR for gene expression analysis is effective for screening multiple genes of interest but limiting because it examines the entire DRG, potentially diluting the effects of nociceptors which are just a subset of the neuron types. Therefore, the effects of disc injury and axonal dieback compounds on DRG sensitization within nociceptors may potentially be diluted or undetected here. Additional characterization of pro-nociceptive and pro-inflammatory mediators expression in DRGs and discs using more precise techniques such as *in situ* hybridization methods is needed to fully understand the crosstalk between these tissues in contributing to pain-signaling modulation.

In addition to neural inflammation and sensitization, it can also be argued that the incomplete recovery of grip strength to baseline is due to the lack of robust disc denervation in all regions of the disc because there is still positive staining for PGP and CGRP in the dorsal AF and the outer 1/3 ventral AF, especially after Vcr injection (Figs. 11,12). This could be that axonal dieback compounds may not be fully penetrating throughout the disc into all regions and therefore, not all nerve fibers were destroyed in the disc. Because only three 40 μm motion segments were processed and analyzed from each animal in this study, these findings should also be interpreted with caution. Further analyses into more motion segment sections will be conducted to provide a more complete representation of how Pyr and Vcr impact nerves throughout the disc.

Reflexive pain behavior from evoked pain assays may not be clinically relevant since most patients with pathological pain conditions frequently report spontaneous pain [116,117]. Hence, movement-evoked pain behavior assays without experimenter control such as open field test and gait analysis were investigated in this study to potentially increase clinical transability of this model of disc-associated LBP. Open field test analysis did not detect significant differences in distance travelled, frequency in the center zone, turn angle, and rearing and grooming behavior between Sham and Injured animals at all timepoints in this study, suggesting the animals did not exhibit movement-evoked pain-like behavior due to disc injury or injections with axonal dieback compounds (Fig. 7). Interestingly, the distance travelled in open field test significantly decreased over time ($p < 0.0001$) which is consistent with previous work by Millecamps *et al*. [118] where they observed reduction in activity and distance travelled of SPARC-null mice with disc-associated pain in open field test [119]. The decline in activity over time, rather than differences between groups, suggests that the age of the rats could influence their exploratory behavior in the open field test.

Another finding is that spatiotemporal gait for both hind and forelimbs are unaltered between Sham and all Injured groups across all weeks (Figs. 8,9,10). Our results align with another model of disc-associated LBP in male rats indicating no changes in base of support gait measurement after 7 weeks post-injury [120]. Gait asymmetry is commonly observed with disc herniation or nerve injury models where there is radiating pain down the limb [121–124]. The absence of these gait abnormalities is a positive sign that the axonal dieback compounds did not induce nerve injury around the disc or cause radiating pain.

This work possesses some limitations that can be addressed in future research. In this study, the *in vivo* studies were exclusively examined in female Sprague Dawley rats, raising the question of potential sex-based differences in the involvement of axonal dieback compounds and denervation in treating pain-like behavior. Without fully understanding the mechanisms and compound interactions, distribution and duration in the disc, there may be challenges translating our findings in clinical research. The time course of disc innervation post-disc injury remains unknown, underscoring the significance of accounting for the timing of interventions in forthcoming studies. Future investigations should also explore the impact of different doses and treatment durations of axonal dieback compounds on axonal retraction and DRG gene expression. Characterization studies of drug distribution in degenerated discs after injection and optimization of alternative drug delivery methods could potentially enhance and prolong the pain alleviation efficacy of axonal dieback compounds.

Conclusions

This research lays the groundwork for investigating axonal dieback compounds, such as Pyr and Vcr, as potential alternative treatments for alleviating pain caused by aberrant nerve growth in discs. In conclusion, the safety of Pyr and Vcr as axonal dieback compounds is affirmed, and these compounds partially alleviate pain in a disc-associated LBP model, with Pyr demonstrating the removal of nerve fibers in part of the discs and Vcr demonstrating reduced DRG sensitization and inflammation. These early findings suggest further research to fully uncover the potential efficacy of Pyr and Vcr in treating disc-associated LBP.

List of Abbreviations

μCT, micro-computed tomography; AF, annulus fibrosus; AGATHA, Automated Gait Analysis Through Hues and Areas; ANOVA, Analysis of Variance; CGRP, Calcitonin gene-related peptide; dAF, dorsal annulus fibrosus; DAPI, 4′,6-diamidino-2-phenylindole; DL, dorsal ligament; DRGs, dorsal root ganglia; FDA, United States Food and Drug Administration; GABA, gamma-aminobutyric acid; GAITOR, Gait Analysis Instrumentation and Technology Optimized for Rodents; Gran, granulation tissue; H&E, hematoxylin and eosin; HU, Hounsfield units; IHC, immunohistochemistry; LBP, low back pain; MAPK, mitogen-activated protein kinase; MQH_2O, MilliQ water; MRI, magnetic resonance imaging; NIH, National Institutes of Health; NP, nucleus pulposus; NSAIDs, nonsteroidal anti-inflammatory drugs; NSF, National Science Foundation; PBS, phosphate-buffered saline; PGP9.5, protein gene product 9.5; PGP, protein gene product; Pyr, pyridoxine; qPCR, quantitative polymerase chain reaction; PCR, polymerase chain reaction; ROI, region of interest; SARM1, sterile alpha and toll/interleukin-1 receptor motif-containing 1; *TRPV1*, transient receptor potential vanilloid 1; ULAM, University of Michigan Unit of Laboratory Animal Medicine; vAF, ventral annulus fibrosus; Vcr, vincristine; VL, ventral ligament; PFA, paraformaldehyde; cDNA, complementary DNA; CT, computed tomography; *ACTB*, β-Actin; *TRPA1*, transient receptor potential ankyrin 1; *Piezo2*, piezo type mechanosensitive ion channel component 2; *Scn9a*, voltage-gated sodium channel Nav1.7; *CHRNA3*, cholinergic receptor nicotinic alpha 3 subunit; *PTGER2*, receptor for prostaglandin E2; *Bdkrb1*, bradykinin receptor b1; *NGF*, nerve growth factor; Inj, Injured; op, operatively.

Availability of Data and Materials

The data that support the findings of this study are available from the corresponding author, RAW, upon reasonable request.

Author Contributions

FL and RAW conceptualized and designed the research study. FL, SMC, CJC, ECB, KDA and RAW acquired and analyzed data. CJC and KDA provided help and advice on gait analysis interpretation. All authors contributed to editorial changes in the manuscript. All authors read and approved the final manuscript. All authors have participated sufficiently in the work and agreed to be accountable for all aspects of the work.

Ethics Approval and Consent to Participate

All animal experiments were in accordance with the National Institute of Health guidelines following Public Health Safety policy on Humane Care and Use of Laboratory Animals and approved by the Institutional Animal Care and Use Committee at the University of Nebraska-Lincoln according to protocol number 2477.

Acknowledgments

We would like to acknowledge Anna Fitzwater, Senior Clinical Veterinarian from University of Nebraska-Lincoln, for her skills and expertise in performing animal surgeries. We would also like to acknowledge the entire staff at the Life Sciences Annex at the University of Nebraska-Lincoln for providing animal care. We acknowledge Richard Bell, postdoctoral fellow from Hospital for Special Surgery for his time and efforts with collecting the brightfield images of the H&E stained L5–L6 motion segments. Special acknowledgements to Anna Levorson, Furqan Mahdi and Jordan Bollinger for their dedication and expert analysis in scoring H&E images, to Anjeza Erickson for analyzing μCT images and quantifying disc volume, to Lydia Saltz for analyzing open field test videos and Uyen Nguyen for assistance in animal acclimation and H&E histology from the Safety study.

Funding

This research was funded by the National Science Foundation (NSF) CAREER Award 1846857.

Conflict of Interest

The authors declare no conflict of interest.

Supplementary Material

Supplementary material associated with this article can be found, in the online version, at https://doi.org/10.22203/eCM.v051a01.

References

[1] Balagué F, Mannion AF, Pellisé F, Cedraschi C. Non-specific low back pain. Lancet. 2012; 379: 482–491. https://doi.org/10.1016/S0140-6736(11)60610-7.

[2] GBD 2015 Disease and Injury Incidence and Prevalence Collaborators. Global, regional, and national incidence, prevalence, and years lived with disability for 310 diseases and injuries, 1990–2015: a systematic analysis for the Global Burden of Disease Study 2015. Lancet. 2016; 388: 1545–1602. https://doi.org/10.1016/S0140-6736(16)31678-6.

[3] Driscoll T, Jacklyn G, Orchard J, Passmore E, Vos T, Freedman G, *et al*. The global burden of occupationally related low back pain: estimates from the Global Burden of Disease 2010 study. Annals of the Rheumatic Diseases. 2014; 73: 975–981. https://doi.org/10.1136/annrheumdis-2013-204631.

[4] Gore M, Sadosky A, Stacey BR, Tai KS, Leslie D. The burden of chronic low back pain: clinical comorbidities, treatment patterns, and health care costs in usual care settings. Spine. 2012; 37: E668–E677. https://doi.org/10.1097/BRS.0b013e318241e5de.

[5] Chaparro LE, Furlan AD, Deshpande A, Mailis-Gagnon A, Atlas S, Turk DC. Opioids compared with placebo or other treatments for chronic low back pain: an update of the Cochrane Review. Spine. 2014; 39: 556–563. https://doi.org/10.1097/BRS.0000000000000249.

[6] Bindu S, Mazumder S, Bandyopadhyay U. Non-steroidal anti-inflammatory drugs (NSAIDs) and organ damage: A current perspective. Biochemical Pharmacology. 2020; 180: 114147. https://doi.org/10.1016/j.bcp.2020.114147.

[7] Vane JR, Botting RM. Anti-inflammatory drugs and their mechanism of action. Inflammation Research: Official Journal of the European Histamine Research Society ... [*et al*.]. 1998; 47: S78–S87. https://doi.org/10.1007/s000110050284.

[8] Singh G, Triadafilopoulos G. Epidemiology of NSAID induced gastrointestinal complications. The Journal of Rheumatology. Supplement. 1999; 56: 18–24.

[9] Laine L, Curtis SP, Cryer B, Kaur A, Cannon CP. Risk factors for NSAID-associated upper GI clinical events in a long-term prospective study of 34 701 arthritis patients. Alimentary Pharmacology & Therapeutics. 2010; 32: 1240–1248. https://doi.org/10.1111/j.1365-2036.2010.04465.x.

[10] Bjarnason I, Hayllar J, MacPherson AJ, Russell AS. Side effects of nonsteroidal anti-inflammatory drugs on the small and large intestine in humans. Gastroenterology. 1993; 104: 1832–1847. https://doi.org/10.1016/0016-5085(93)90667-2.

[11] Whelton A, Watson AJ. Nonsteroidal anti-inflammatory drugs: effects on kidney function. Clinical Nephrotoxins. 1998; 203–216. https://doi.org/10.1007/978-94-015-9088-4_14.

[12] Ray WA, Stein CM, Daugherty JR, Hall K, Arbogast PG, Griffin MR. COX-2 selective non-steroidal anti-inflammatory drugs and risk of serious coronary heart disease. Lancet. 2002; 360: 1071–1073. https://doi.org/10.1016/S0140-6736(02)11131-7.

[13] Page J, Henry D. Consumption of NSAIDs and the development of congestive heart failure in elderly patients: an underrecognized public health problem. Archives of Internal Medicine. 2000; 160: 777–784. https://doi.org/10.1001/archinte.160.6.777.

[14] Ivanova JI, Birnbaum HG, Schiller M, Kantor E, Johnstone BM, Swindle RW. Real-world practice patterns, health-care utilization, and costs in patients with low back pain: the long road to guideline-concordant care. The Spine Journal: Official Journal of the North American Spine Society. 2011; 11: 622–632. https://doi.org/10.1016/j.spinee.2011.03.017.

[15] Deyo RA, Von Korff M, Duhrkoop D. Opioids for low back pain. BMJ: British Medical Journal/British Medical Association. 2015; 350: g6380. https://doi.org/10.1136/bmj.g6380.

[16] Cheatle MD. Prescription Opioid Misuse, Abuse, Morbidity, and Mortality: Balancing Effective Pain Management and Safety. Pain Medicine: the Official Journal of the American Academy of Pain Medicine. 2015; 16: S3–S8. https://doi.org/10.1111/pme.12904.

[17] Brantigan JW, Neidre A, Toohey JS. The Lumbar I/F Cage for posterior lumbar interbody fusion with the variable screw placement system: 10-year results of a Food and Drug Administration clinical trial. The Spine Journal: Official Journal of the North Ameri-

can Spine Society. 2004; 4: 681–688. https://doi.org/10.1016/j.spinee.2004.05.253.

[18] García-Cosamalón J, del Valle ME, Calavia MG, García-Suárez O, López-Muñiz A, Otero J, *et al*. Intervertebral disc, sensory nerves and neurotrophins: who is who in discogenic pain? Journal of Anatomy. 2010; 217: 1–15. https://doi.org/10.1111/j.1469-7580.2010.01227.x.

[19] Binch AL, Cole AA, Breakwell LM, Michael AL, Chiverton N, Creemers LB, *et al*. Nerves are more abundant than blood vessels in the degenerate human intervertebral disc. Arthritis Research & Therapy. 2015; 17: 370. https://doi.org/10.1186/s13075-015-0889-6.

[20] Freemont AJ, Peacock TE, Goupille P, Hoyland JA, O'Brien J, Jayson MI. Nerve ingrowth into diseased intervertebral disc in chronic back pain. Lancet. 1997; 350: 178–181. https://doi.org/10.1016/s0140-6736(97)02135-1.

[21] Johnson WEB, Caterson B, Eisenstein SM, Hynds DL, Snow DM, Roberts S. Human intervertebral disc aggrecan inhibits nerve growth *in vitro*. Arthritis and Rheumatism. 2002; 46: 2658–2664. https://doi.org/10.1002/art.10585.

[22] Lama P, Le Maitre CL, Harding IJ, Dolan P, Adams MA. Nerves and blood vessels in degenerated intervertebral discs are confined to physically disrupted tissue. Journal of Anatomy. 2018; 233: 86–97. https://doi.org/10.1111/joa.12817.

[23] Ozawa T, Ohtori S, Inoue G, Aoki Y, Moriya H, Takahashi K. The degenerated lumbar intervertebral disc is innervated primarily by peptide-containing sensory nerve fibers in humans. Spine. 2006; 31: 2418–2422. https://doi.org/10.1097/01.brs.0000239159.74211.9c.

[24] Risbud MV, Shapiro IM. Role of cytokines in intervertebral disc degeneration: pain and disc content. Nature Reviews. Rheumatology. 2014; 10: 44–56. https://doi.org/10.1038/nrrheum.2013.160.

[25] Cook AD, Christensen AD, Tewari D, McMahon SB, Hamilton JA. Immune Cytokines and Their Receptors in Inflammatory Pain. Trends in Immunology. 2018; 39: 240–255. https://doi.org/10.1016/j.it.2017.12.003.

[26] Nachemson A. Towards a better understanding of low-back pain: a review of the mechanics of the lumbar disc. Rheumatology and Rehabilitation. 1975; 14: 129–143. https://doi.org/10.1093/rheumatology/14.3.129.

[27] Wang S, Wang S, Asgar J, Joseph J, Ro JY, Wei F, *et al*. Ca^{2+} and calpain mediate capsaicin-induced ablation of axonal terminals expressing transient receptor potential vanilloid 1. The Journal of Biological Chemistry. 2017; 292: 8291–8303. https://doi.org/10.1074/jbc.M117.778290.

[28] Reilly DM, Ferdinando D, Johnston C, Shaw C, Buchanan KD, Green MR. The epidermal nerve fibre network: characterization of nerve fibres in human skin by confocal microscopy and assessment of racial variations. The British Journal of Dermatology. 1997; 137: 163–170. https://doi.org/10.1046/j.1365-2133.1997.18001893.x.

[29] Nolano M, Simone DA, Wendelschafer-Crabb G, Johnson T, Hazen E, Kennedy WR. Topical capsaicin in humans: parallel loss of epidermal nerve fibers and pain sensation. Pain. 1999; 81: 135–145. https://doi.org/10.1016/s0304-3959(99)00007-x.

[30] Simone DA, Baumann TK, LaMotte RH. Dose-dependent pain and mechanical hyperalgesia in humans after intradermal injection of capsaicin. Pain. 1989; 38: 99–107. https://doi.org/10.1016/0304-3959(89)90079-1.

[31] Simpson DM, Robinson-Papp J, Van J, Stoker M, Jacobs H, Snijder RJ, *et al*. Capsaicin 8 % Patch in Painful Diabetic Peripheral Neuropathy: A Randomized, Double-Blind, Placebo-Controlled Study. The Journal of Pain. 2017; 18: 42–53. https://doi.org/10.1016/j.jpain.2016.09.008.

[32] Simpson DM, Brown S, Tobias J, NGX-4010 C107 Study Group. Controlled trial of high-concentration capsaicin patch for treatment of painful HIV neuropathy. Neurology. 2008; 70: 2305–2313. https://doi.org/10.1212/01.wnl.0000314647.35825.9c.

[33] Wallace M, Pappagallo M. Qutenza®: a capsaicin 8 % patch for the management of postherpetic neuralgia. Expert Review of Neurotherapeutics. 2011; 11: 15–27. https://doi.org/10.1586/ern.10.182.

[34] Campbell CM, Diamond E, Schmidt WK, Kelly M, Allen R, Houghton W, *et al*. A randomized, double-blind, placebo-controlled trial of injected capsaicin for pain in Morton's neuroma. Pain. 2016; 157: 1297–1304. https://doi.org/10.1097/j.pain.0000000000000544.

[35] Stevens RM, Ervin J, Nezzer J, Nieves Y, Guedes K, Burges R, *et al*. Randomized, Double-Blind, Placebo-Controlled Trial of Intraarticular Trans-Capsaicin for Pain Associated With Osteoarthritis of the Knee. Arthritis & Rheumatology. 2019; 71: 1524–1533. https://doi.org/10.1002/art.40894.

[36] Cantillon M, Vause E, Sykes D, Russell R, Moon A, Hughes S. Preliminary safety, tolerability and efficacy of ALGRX 4975 in osteoarthritis (OA) of the knee. The Journal of Pain. 2005; 6: S39. https://doi.org/10.1016/j.jpain.2005.01.152.

[37] Vutskits L, Briner A, Klauser P, Gascon E, Dayer AG, Kiss JZ, *et al*. Adverse effects of methylene blue on the central nervous system. Anesthesiology. 2008; 108: 684–692. https://doi.org/10.1097/ALN.0b013e3181684be4.

[38] Li JW, Wang RL, Xu J, Sun KY, Jiang HM, Sun ZY, *et al*. Methylene blue prevents osteoarthritis progression and relieves pain in rats via upregulation of Nrf2/PRDX1. Acta Pharmacologica Sinica. 2022; 43: 417–428. https://doi.org/10.1038/s41401-021-00646-z.

[39] Huang C, Tong L, Lu X, Wang J, Yao W, Jiang B, *et al*. Methylene Blue Attenuates iNOS Induction Through Suppression of Transcriptional Factor Binding Amid iNOS mRNA Transcription. Journal of Cellular Biochemistry. 2015; 116: 1730–1740. https://doi.org/10.1002/jcb.25132.

[40] Peng B, Zhang Y, Hou S, Wu W, Fu X. Intradiscal methylene blue injection for the treatment of chronic discogenic low back pain. European Spine Journal: Official Publication of the European Spine Society, the European Spinal Deformity Society, and the European Section of the Cervical Spine Research Society. 2007; 16: 33–38. https://doi.org/10.1007/s00586-006-0076-1.

[41] Kallewaard JW, Wintraecken VM, Geurts JW, Willems PC, van Santbrink H, Terwiel CTM, *et al*. A multicenter randomized controlled trial on the efficacy of intradiscal methylene blue injection for chronic discogenic low back pain: the IMBI study. Pain. 2019; 160: 945–953. https://doi.org/10.1097/j.pain.0000000000001475.

[42] Wang X, Zhang S, Xie Z, Chen L, Yang B, Wu X. Deleterious Effects of Methylene Blue on Rat Nucleus Pulposus Cell *In Vitro*: Changes in Cell Viability and Secretory Phenotype in Exposed Cells. Journal of Neurological Surgery. Part A, Central European Neurosurgery 2019; 80: 174–179. https://doi.org/10.1055/s-0038-1670638.

[43] Zhang L, Liu Y, Huang Z, Nan L, Wang F, Zhou S, *et al*. Toxicity effects of methylene blue on rat intervertebral disc annulus fibrosus cells. Pain Physician. 2019; 22: 155–164.

[44] Baxter P. Pyridoxine-dependent and pyridoxine-responsive seizures. Developmental Medicine and Child Neurology. 2001; 43: 416–420. https://doi.org/10.1111/j.1469-8749.2001.tb00231.x.

[45] Kashanian M, Mazinani R, Jalalmanesh S, Babayanzad Ahari S. Pyridoxine (vitamin B6) therapy for premenstrual syndrome. International Journal of Gynaecology and Obstetrics: the Official Organ of the International Federation of Gynaecology and Obstetrics. 2007; 96: 43–44. https://doi.org/10.1016/j.ijgo.2006.09.014.

[46] Ghavanini AA, Kimpinski K. Revisiting the evidence for neuropathy caused by pyridoxine deficiency and excess. Journal of Clinical Neuromuscular Disease. 2014; 16: 25–31. https://doi.org/10.1097/CND.0000000000000049.

[47] Schaumburg H, Kaplan J, Windebank A, Vick N, Rasmus S, Pleasure D, *et al*. Sensory neuropathy from pyridoxine abuse. A new megavitamin syndrome. The New England Journal of Medicine. 1983; 309: 445–448. https://doi.org/10.1056/NEJM198308253090801.

[48] Chung JY, Choi JH, Hwang CY, Youn HY. Pyridoxine induced neuropathy by subcutaneous administration in dogs. Journal of Veteri-

nary Science. 2008; 9: 127–131. https://doi.org/10.4142/jvs.2008.9.2.127.

[49] Montpetit VJ, Clapin DF, Tryphonas L, Dancea S. Alteration of neuronal cytoskeletal organization in dorsal root ganglia associated with pyridoxine neurotoxicity. Acta Neuropathologica. 1988; 76: 71–81. https://doi.org/10.1007/BF00687682.

[50] Hadtstein F, Vrolijk M. Vitamin B-6-Induced Neuropathy: Exploring the Mechanisms of Pyridoxine Toxicity. Advances in Nutrition. 2021; 12: 1911–1929. https://doi.org/10.1093/advances/nmab033.

[51] Mora E, Smith EML, Donohoe C, Hertz DL. Vincristine-induced peripheral neuropathy in pediatric cancer patients. American Journal of Cancer Research. 2016; 6: 2416–2430.

[52] Macfarlane BV, Wright A, Benson HA. Reversible blockade of retrograde axonal transport in the rat sciatic nerve by vincristine. The Journal of Pharmacy and Pharmacology. 1997; 49: 97–101. https://doi.org/10.1111/j.2042-7158.1997.tb06759.x.

[53] LaPointe NE, Morfini G, Brady ST, Feinstein SC, Wilson L, Jordan MA. Effects of eribulin, vincristine, paclitaxel and ixabepilone on fast axonal transport and kinesin-1 driven microtubule gliding: implications for chemotherapy-induced peripheral neuropathy. Neurotoxicology. 2013; 37: 231–239. https://doi.org/10.1016/j.neuro.2013.05.008.

[54] Tanner KD, Levine JD, Topp KS. Microtubule disorientation and axonal swelling in unmyelinated sensory axons during vincristine-induced painful neuropathy in rat. Journal of Comparative Neurology. 1998; 395: 481–492. https://doi.org/10.1002/(SICI)1096-9861(19980615)395:4<481::AID-CNE5>3.0.CO;2-Y.

[55] Topp KS, Tanner KD, Levine JD. Damage to the cytoskeleton of large diameter sensory neurons and myelinated axons in vincristine-induced painful peripheral neuropathy in the rat. Journal of Comparative Neurology. 2000; 424: 563–576. https://doi.org/10.1002/1096-9861(20000904)424:4<563::AID-CNE1>3.0.CO;2-U.

[56] Djaldetti R, Hart J, Alexandrova S, Cohen S, Beilin BZ, Djaldetti M, *et al*. Vincristine-induced alterations in Schwann cells of mouse peripheral nerve. American Journal of Hematology. 1996; 52: 254–257. https://doi.org/10.1002/(SICI)1096-8652(199608)52:4<254::AID-AJH3>3.0.CO;2-R.

[57] Geisler S, Doan RA, Cheng GC, Cetinkaya-Fisgin A, Huang SX, Höke A, *et al*. Vincristine and bortezomib use distinct upstream mechanisms to activate a common SARM1-dependent axon degeneration program. JCI Insight. 2019; 4: e129920. https://doi.org/10.1172/jci.insight.129920.

[58] Zhou L, Ao L, Yan Y, Li C, Li W, Ye A, *et al*. Levo-corydalmine Attenuates Vincristine-Induced Neuropathic Pain in Mice by Up-regulating the Nrf2/HO-1/CO Pathway to Inhibit Connexin 43 Expression. Neurotherapeutics: the Journal of the American Society for Experimental NeuroTherapeutics. 2020; 17: 340–355. https://doi.org/10.1007/s13311-019-00784-7.

[59] Bacharach R, Lowden M, Ahmed A. Pyridoxine Toxicity Small Fiber Neuropathy with Dysautonomia: A Case Report. Journal of Clinical Neuromuscular Disease. 2017; 19: 43–46. https://doi.org/10.1097/CND.0000000000000172.

[60] Chaudary AN, Porter-Blake A, Holford P. Indices of pyridoxine levels on symptoms associated with toxicity: a retrospective study. Journal of Orthomolecular Medicine. 2003; 18: 65–76.

[61] Lee FS, Nguyen UN, Munns EJ, Wachs RA. Screening for axonal retraction and cytotoxicity using dorsal root ganglia explants to treat pain caused by aberrant nerve sprouting. 2023. (preprint) https://doi.org/10.21203/rs.3.rs-2987056/v1.

[62] Lillyman DJ, Lee FS, Barnett EC, Miller TJ, Alvaro ML, Drvol HC, *et al*. Axial hypersensitivity is associated with aberrant nerve sprouting in a novel model of disc degeneration in female Sprague Dawley rats. JOR Spine. 2022; 5: e1212. https://doi.org/10.1002/jsp2.1212.

[63] Kwack EK, Kim DJ, Park TI, Cho KR, Kwon IH, Sohn YK. Neural toxicity induced by accidental intrathecal vincristine administration. Journal of Korean Medical Science. 1999; 14: 688–692. https://doi.org/10.3346/jkms.1999.14.6.688.

[64] Hennipman B, de Vries E, Bökkerink JP, Ball LM, Veerman AJ. Intrathecal vincristine: 3 fatal cases and a review of the literature. Journal of Pediatric Hematology/Oncology. 2009; 31: 816–819. https://doi.org/10.1097/MPH.0b013e3181b83fba.

[65] Michigan Uo. ULAM pain assessment in rats.pdf: Research A to Z. 2015. Available at: https://az.research.umich.edu/file/1255 (Accessed: 23 October 2023).

[66] Lai A, Gansau J, Gullbrand SE, Crowley J, Cunha C, Dudli S, *et al*. Development of a standardized histopathology scoring system for intervertebral disc degeneration in rat models: An initiative of the ORS spine section. JOR Spine. 2021; 4: e1150. https://doi.org/10.1002/jsp2.1150.

[67] Schneider CA, Rasband WS, Eliceiri KW. NIH Image to ImageJ: 25 years of image analysis. Nature Methods. 2012; 9: 671–675. https://doi.org/10.1038/nmeth.2089.

[68] Millecamps M, Czerminski JT, Mathieu AP, Stone LS. Behavioral signs of axial low back pain and motor impairment correlate with the severity of intervertebral disc degeneration in a mouse model. The Spine Journal: Official Journal of the North American Spine Society. 2015; 15: 2524–2537. https://doi.org/10.1016/j.spinee.2015.08.055.

[69] Wang D, Lai A, Gansau J, Seifert AC, Munitz J, Zaheer K, *et al*. Lumbar endplate microfracture injury induces Modic-like changes, intervertebral disc degeneration and spinal cord sensitization—an *in vivo* rat model. The Spine Journal: Official Journal of the North American Spine Society. 2023; 23: 1375–1388. https://doi.org/10.1016/j.spinee.2023.04.012.

[70] Bachem A. The modified Fechner-Weber law as a complex law of dose-action. The American Journal of Psychology. 1956; 69: 588–603. https://doi.org/10.2307/1419082.

[71] Tappe-Theodor A, Kuner R. Studying ongoing and spontaneous pain in rodents—challenges and opportunities. The European Journal of Neuroscience. 2014; 39: 1881–1890. https://doi.org/10.1111/ejn.12643.

[72] Jacobs BY, Lakes EH, Reiter AJ, Lake SP, Ham TR, Leipzig ND, *et al*. The Open Source GAITOR Suite for Rodent Gait Analysis. Scientific Reports. 2018; 8: 9797. https://doi.org/10.1038/s41598-018-28134-1.

[73] Grabovskaya SV, Salyha YT. Do Results of the Open Field Test Depend on the Arena Shape? Neurophysiology. 2014; 46: 376–380. https://doi.org/10.1007/s11062-014-9458-x.

[74] Deuis JR, Dvorakova LS, Vetter I. Methods Used to Evaluate Pain Behaviors in Rodents. Frontiers in Molecular Neuroscience. 2017; 10: 284. https://doi.org/10.3389/fnmol.2017.00284.

[75] Jacobs BY, Dunnigan K, Pires-Fernandes M, Allen KD. Unique spatiotemporal and dynamic gait compensations in the rat monoiodoacetate injection and medial meniscus transection models of knee osteoarthritis. Osteoarthritis and Cartilage/OARS, Osteoarthritis Research Society. 2017; 25: 750–758. https://doi.org/10.1016/j.joca.2016.12.012.

[76] Kloefkorn HE, Pettengill TR, Turner SM, Streeter KA, Gonzalez-Rothi EJ, Fuller DD, *et al*. Automated Gait Analysis Through Hues and Areas (AGATHA): A Method to Characterize the Spatiotemporal Pattern of Rat Gait. Annals of Biomedical Engineering. 2017; 45: 711–725. https://doi.org/10.1007/s10439-016-1717-0.

[77] Lillyman DJ, Barnett EC, Miller TJ, Wachs RA. Application of microcomputed tomography to calculate rat intervertebral disc volume as a surrogate measure of degeneration. Computer Methods in Biomechanics and Biomedical Engineering: Imaging & Visualization. 2023; 11: 1717–1723. https://doi.org/10.1080/21681163.2023.2182607.

[78] Batawil N, Sabiq S. Hounsfield unit for the diagnosis of bone mineral density disease: a proof of concept study. Radiography. 2016; 22: e93–e98. https://doi.org/10.1016/j.radi.2015.11.004.

[79] Molteni R. Prospects and challenges of rendering tissue density in Hounsfield units for cone beam computed tomography. Oral Surgery,

Oral Medicine, Oral Pathology and Oral Radiology. 2013; 116: 105–119. https://doi.org/10.1016/j.oooo.2013.04.013.

[80] Mohd Isa IL, Abbah SA, Kilcoyne M, Sakai D, Dockery P, Finn DP, *et al*. Implantation of hyaluronic acid hydrogel prevents the pain phenotype in a rat model of intervertebral disc injury. Science Advances. 2018; 4: eaaq0597. https://doi.org/10.1126/sciadv.aaq0597.

[81] Aoki Y, Takahashi Y, Ohtori S, Moriya H, Takahashi K. Distribution and immunocytochemical characterization of dorsal root ganglion neurons innervating the lumbar intervertebral disc in rats: a review. Life Sciences. 2004; 74: 2627–2642. https://doi.org/10.1016/j.lfs.2004.01.008.

[82] Bankhead P, Loughrey MB, Fernández JA, Dombrowski Y, McArt DG, Dunne PD, *et al.* QuPath: Open source software for digital pathology image analysis. Scientific Reports. 2017; 7: 16878. https://doi.org/10.1038/s41598-017-17204-5.

[83] Ding F, Shao ZW, Xiong LM. Cell death in intervertebral disc degeneration. Apoptosis: an International Journal on Programmed Cell Death. 2013; 18: 777–785. https://doi.org/10.1007/s10495-013-0839-1.

[84] Jang K, Garraway SM. A review of dorsal root ganglia and primary sensory neuron plasticity mediating inflammatory and chronic neuropathic pain. Neurobiology of Pain. 2024; 15: 100151. https://doi.org/10.1016/j.ynpai.2024.100151.

[85] Morinaga T, Takahashi K, Yamagata M, Chiba T, Tanaka K, Takahashi Y, *et al*. Sensory innervation to the anterior portion of lumbar intervertebral disc. Spine. 1996; 21: 1848–1851. https://doi.org/10.1097/00007632-199608150-00002.

[86] Sameda H, Takahashi Y, Takahashi K, Chiba T, Ohtori S, Moriya H. Dorsal root ganglion neurones with dichotomising afferent fibres to both the lumbar disc and the groin skin. A possible neuronal mechanism underlying referred groin pain in lower lumbar disc diseases. The Journal of Bone and Joint Surgery. British Volume. 2003; 85: 600–603. https://doi.org/10.1302/0301-620x.85b4.13306.

[87] Goni R, García P, Foissac S. The qPCR data statistical analysis. Integromics White Paper. 2009; 1: 1–9.

[88] Reifenrath J, Heider M, Kempfert M, Harting H, Weidemann F, Strauss S, *et al*. Buprenorphine in rats: potent analgesic or trigger for fatal side effects? Acta Veterinaria Scandinavica. 2022; 64: 37. https://doi.org/10.1186/s13028-022-00661-y.

[89] Lipson SJ, Muir H. Experimental intervertebral disc degeneration: Morphologic and proteoglycan changes over time. Arthritis and Rheumatism. 1981; 24: 12–21. https://doi.org/10.1002/art.1780240103.

[90] Barendse GA, van Den Berg SG, Kessels AH, Weber WE, van Kleef M. Randomized controlled trial of percutaneous intradiscal radiofrequency thermocoagulation for chronic discogenic back pain: lack of effect from a 90-second 70 C lesion. Spine. 2001; 26: 287–292. https://doi.org/10.1097/00007632-200102010-00014.

[91] Finch PM, Price LM, Drummond PD. Radiofrequency heating of painful annular disruptions: one-year outcomes. Journal of Spinal Disorders & Techniques. 2005; 18: 6–13. https://doi.org/10.1097/01.bsd.0000143312.08303.5d.

[92] Kvarstein G, Måwe L, Indahl A, Hol PK, Tennøe B, Digernes R, *et al*. A randomized double-blind controlled trial of intra-annular radiofrequency thermal disc therapy—a 12-month follow-up. Pain. 2009; 145: 279–286. https://doi.org/10.1016/j.pain.2009.05.001.

[93] Zhang L, Ding XL, Zhao XL, Wang JN, Li YP, Tian M. Fluoroscopy-guided Bipolar Radiofrequency Thermocoagulation Treatment for Discogenic Low Back Pain. Chinese Medical Journal. 2016; 129: 2313–2318. https://doi.org/10.4103/0366-6999.190682.

[94] Saal JA, Saal JS. Intradiscal electrothermal treatment for chronic discogenic low back pain: prospective outcome study with a minimum 2-year follow-up. Spine. 2002; 27: 966–974. https://doi.org/10.1097/00007632-200205010-00017.

[95] Peng B, Pang X, Wu Y, Zhao C, Song X. A randomized placebo-controlled trial of intradiscal methylene blue injection for the treatment of chronic discogenic low back pain. Pain. 2010; 149: 124–129. https://doi.org/10.1016/j.pain.2010.01.021.

[96] Kim SH, Ahn SH, Cho YW, Lee DG. Effect of Intradiscal Methylene Blue Injection for the Chronic Discogenic Low Back Pain: One Year Prospective Follow-up Study. Annals of Rehabilitation Medicine. 2012; 36: 657–664. https://doi.org/10.5535/arm.2012.36.5.657.

[97] Gupta G, Radhakrishna M, Chankowsky J, Asenjo JF. Methylene blue in the treatment of discogenic low back pain. Pain Physician. 2012; 15: 333–338.

[98] Kallewaard JW, Geurts JW, Kessels A, Willems P, van Santbrink H, van Kleef M. Efficacy, Safety, and Predictors of Intradiscal Methylene Blue Injection for Discogenic Low Back Pain: Results of a Multicenter Prospective Clinical Series. Pain Practice: the Official Journal of World Institute of Pain. 2016; 16: 405–412. https://doi.org/10.1111/papr.12283.

[99] Zhang X, Hao J, Hu Z, Yang H. Clinical Evaluation and Magnetic Resonance Imaging Assessment of Intradiscal Methylene Blue Injection for the Treatment of Discogenic Low Back Pain. Pain Physician. 2016; 19: E1189–E1195.

[100] Levi DS, Horn S, Walko E. Intradiskal methylene blue treatment for diskogenic low back pain. PM & R: the Journal of Injury, Function, and Rehabilitation. 2014; 6: 1030–1037. https://doi.org/10.1016/j.pmrj.2014.04.008.

[101] Freedman BA, Cohen SP, Kuklo TR, Lehman RA, Larkin P, Giuliani JR. Intradiscal electrothermal therapy (IDET) for chronic low back pain in active-duty soldiers: 2-year follow-up. The Spine Journal: Official Journal of the North American Spine Society. 2003; 3: 502–509. https://doi.org/10.1016/j.spinee.2003.07.010.

[102] Spruit M, Jacobs WCH. Pain and function after intradiscal electrothermal treatment (IDET) for symptomatic lumbar disc degeneration. European Spine Journal: Official Publication of the European Spine Society, the European Spinal Deformity Society, and the European Section of the Cervical Spine Research Society. 2002; 11: 589–593. https://doi.org/10.1007/s00586-002-0450-6.

[103] Davis TT, Delamarter RB, Sra P, Goldstein TB. The IDET procedure for chronic discogenic low back pain. Spine. 2004; 29: 752–756. https://doi.org/10.1097/01.brs.0000119403.11472.40.

[104] Ohtori S, Takahashi K, Chiba T, Yamagata M, Sameda H, Moriya H. Substance P and calcitonin gene-related peptide immunoreactive sensory DRG neurons innervating the lumbar intervertebral discs in rats. Annals of Anatomy = Anatomischer Anzeiger: Official Organ of the Anatomische Gesellschaft. 2002; 184: 235–240. https://doi.org/10.1016/S0940-9602(02)80113-3.

[105] Aoki Y, Ohtori S, Takahashi K, Ino H, Takahashi Y, Chiba T, *et al*. Innervation of the lumbar intervertebral disc by nerve growth factor-dependent neurons related to inflammatory pain. Spine. 2004; 29: 1077–1081. https://doi.org/10.1097/00007632-200405150-00005.

[106] Zhang S, Hu B, Liu W, Wang P, Lv X, Chen S, *et al*. The role of structure and function changes of sensory nervous system in intervertebral disc-related low back pain. Osteoarthritis and Cartilage/OARS, Osteoarthritis Research Society. 2021; 29: 17–27. https://doi.org/10.1016/j.joca.2020.09.002.

[107] Fernihough J, Gentry C, Bevan S, Winter J. Regulation of calcitonin gene-related peptide and TRPV1 in a rat model of osteoarthritis. Neuroscience Letters. 2005; 388: 75–80. https://doi.org/10.1016/j.neulet.2005.06.044.

[108] Obeidat AM, Wood MJ, Adamczyk NS, Ishihara S, Li J, Wang L, *et al*. Piezo2 expressing nociceptors mediate mechanical sensitization in experimental osteoarthritis. Nature Communications. 2023; 14: 2479. https://doi.org/10.1038/s41467-023-38241-x.

[109] McGaraughty S, Chu KL, Perner RJ, Didomenico S, Kort ME, Kym PR. TRPA1 modulation of spontaneous and mechanically evoked firing of spinal neurons in uninjured, osteoarthritic, and inflamed rats. Molecular Pain. 2010; 6: 14. https://doi.org/10.1186/1744-8069-6-14.

[110] Zaki S, Smith MM, Little CB. Pathology-pain relationships in dif-

ferent osteoarthritis animal model phenotypes: it matters what you measure, when you measure, and how you got there. Osteoarthritis and Cartilage/OARS, Osteoarthritis Research Society. 2021; 29: 1448–1461. https://doi.org/10.1016/j.joca.2021.03.023.

[111] Lai A, Iliff D, Zaheer K, Gansau J, Laudier DM, Zachariou V, *et al*. Annulus Fibrosus Injury Induces Acute Neuroinflammation and Chronic Glial Response in Dorsal Root Ganglion and Spinal Cord—An *In Vivo* Rat Discogenic Pain Model. International Journal of Molecular Sciences. 2024; 25: 1762. https://doi.org/10.3390/ijms25031762.

[112] Jang Y, Kim M, Hwang SW. Molecular mechanisms underlying the actions of arachidonic acid-derived prostaglandins on peripheral nociception. Journal of Neuroinflammation. 2020; 17: 30. https://doi.org/10.1186/s12974-020-1703-1.

[113] Driscoll C, Chanalaris A, Knights C, Ismail H, Sacitharan PK, Gentry C, *et al*. Nociceptive Sensitizers Are Regulated in Damaged Joint Tissues, Including Articular Cartilage, When Osteoarthritic Mice Display Pain Behavior. Arthritis & Rheumatology. 2016; 68: 857–867. https://doi.org/10.1002/art.39523.

[114] Shi C, Das V, Li X, Kc R, Qiu S, O-Sullivan I, *et al*. Development of an *in vivo* mouse model of discogenic low back pain. Journal of Cellular Physiology. 2018; 233: 6589–6602. https://doi.org/10.1002/jcp.26280.

[115] Kiguchi N, Maeda T, Kobayashi Y, Saika F, Kishioka S. Involvement of inflammatory mediators in neuropathic pain caused by vincristine. International Review of Neurobiology. 2009; 85: 179–190. https://doi.org/10.1016/S0074-7742(09)85014-9.

[116] Ma L, Liu S, Yi M, Wan Y. Spontaneous pain as a challenge of research and management in chronic pain. Medical Review. 2022; 2: 308–319. https://doi.org/10.1515/mr-2022-0007.

[117] Maier C, Baron R, Tölle TR, Binder A, Birbaumer N, Birklein F, *et al*. Quantitative sensory testing in the German Research Network on Neuropathic Pain (DFNS): somatosensory abnormalities in 1236 patients with different neuropathic pain syndromes. Pain. 2010; 150: 439–450. https://doi.org/10.1016/j.pain.2010.05.002.

[118] Millecamps M, Tajerian M, Naso L, Sage EH, Stone LS. Lumbar intervertebral disc degeneration associated with axial and radiating low back pain in ageing SPARC-null mice. Pain. 2012; 153: 1167–1179. https://doi.org/10.1016/j.pain.2012.01.027.

[119] Lecorps B, Rödel HG, Féron C. Assessment of anxiety in open field and elevated plus maze using infrared thermography. Physiology & Behavior. 2016; 157: 209–216. https://doi.org/10.1016/j.physbeh.2016.02.014.

[120] Muralidharan A, Park TSW, Mackie JT, Gimenez LGS, Kuo A, Nicholson JR, *et al*. Establishment and Characterization of a Novel Rat Model of Mechanical Low Back Pain Using Behavioral, Pharmacologic and Histologic Methods. Frontiers in Pharmacology. 2017; 8: 493. https://doi.org/10.3389/fphar.2017.00493.

[121] Kameda T, Kaneuchi Y, Sekiguchi M, Konno SI. Measurement of mechanical withdrawal thresholds and gait analysis using the CatWalk method in a nucleus pulposus-applied rodent model. Journal of Experimental Orthopaedics. 2017; 4: 31. https://doi.org/10.1186/s40634-017-0105-5.

[122] Shamji MF, Allen KD, So S, Jing L, Adams SB Jr, Schuh R, *et al*. Gait abnormalities and inflammatory cytokines in an autologous nucleus pulposus model of radiculopathy. Spine. 2009; 34: 648–654. https://doi.org/10.1097/BRS.0b013e318197f013.

[123] Isvoranu G, Manole E, Neagu M. Gait Analysis Using Animal Models of Peripheral Nerve and Spinal Cord Injuries. Biomedicines. 2021; 9: 1050. https://doi.org/10.3390/biomedicines9081050.

[124] Heinzel J, Swiadek N, Ashmwe M, Rührnößl A, Oberhauser V, Kolbenschlag J, *et al*. Automated Gait Analysis to Assess Functional Recovery in Rodents with Peripheral Nerve or Spinal Cord Contusion Injury. Journal of Visualized Experiments: JoVE. 2020; e61852. https://doi.org/10.3791/61852.

Editor's note: The Scientific Editor responsible for this paper was Mauro Alini.

Received: 15th February 2024; **Accepted**: 21st August 2024; **Published**: 26th May 2025